



الجامعة الإسلامية العالمية شيتاغونغ  
International Islamic University Chittagong

**BACHELOR OF SCIENCE IN ELECTRONIC AND  
TELECOMMUNICATION ENGINEERING**

**Performance Investigation of Three Precoding Methods for Maximal  
Energy Efficiency in Next Generation Wireless Communications System**

**Supervised By**

Engr. Syed Zahidur Rashid  
Assistant Professor

Department of Electronic and Telecommunication Engineering, IIUC

**Submitted By**

Md. Humayun Kabir  
Matric ID: T141007  
Program: B. Sc. In ETE

**Department of Electronic and Telecommunication Engineering**

International Islamic University Chittagong

Kumira, Sitakunda, Chittagong – 4318

September 2018

# **Performance Investigation of Three Precoding Methods for Maximal Energy Efficiency in Next Generation Wireless Communications System**

**(THIS THESIS REPORT IS SUBMITTED FOR THE PARTIAL FULFILMENT OF THE BACHELOR OF SCIENCE IN ELECTRONIC AND TELECOMMUNICATION ENGINEERING)**

## **Submitted By**

**Md. Humayun Kabir  
Matric ID: T141007  
Program: B. Sc. In ETE**

## **Supervised By**

**Engr. Syed Zahidur Rashid  
Assistant Professor  
Department of Electronic and Telecommunication Engineering, IIUC**



**Department of Electronic and Telecommunication Engineering  
International Islamic University Chittagong  
Kumira, Sitakunda, Chittagong – 4318**

This thesis submitted by **Md Humayun Kabir**, ID No.**T141007** in partial fulfillment of the requirements for the degree of Bachelor of Science in Electronic and Telecommunication Engineering (ETE) and accepted as to style and content by:

**(Dr. Mohammad Sanaullah Chowdhury)**  
Associate Professor, Department of CSE  
University of Chittagong

External Member

**(Engr. Abdul Gafur)**  
Associate Professor  
Dept. of ETE  
International Islamic University Chittagong

Internal Member

**(Engr. Syed Zahidur Rashid)**  
Assistant Professor  
Dept. of ETE  
International Islamic University Chittagong

Internal Member & Supervisor

**(Engr. Mohammed Jashim Uddin)**  
Assistant Professor  
Dept. of ETE  
International Islamic University Chittagong

Chairman

## **Certificate of Approval**

The thesis entitled as “**Performance Investigation of Three Precoding Methods for Maximal Energy Efficiency in Next Generation Wireless Communications System**” submitted by **Md Humayun Kabir** bearing **ID No. T141007**, to the Department of Electronic and Telecommunication Engineering (ETE) of International Islamic University Chittagong (IIUC) has been accepted as satisfactory for the partial fulfillment of the requirements for the Degree of Bachelor in Electronic and Telecommunication Engineering and approved as to its style and contents for the examination held on **4<sup>th</sup> September 2018**.

Approved By-

---

**Engr. Syed Zahidur Rashid**

Supervisor

Assistant Professor

Department of Electronic and Telecommunication Engineering

International Islamic University Chittagong

## DECLARATION OF CANDIDATE

It is hereby declared that the work presented here in is genuine work done by me and has not concurrently submitted in candidature for any degree. The result of the thesis that i have found totally depend on my own investigation/work.

This work was done under the guidance of **Engr. Syed Zahidur Rashid**, Assistant Professor of Electronic and Telecommunication Engineering, International Islamic University Chittagong.

-----  
(Signature of Candidate)

Md. Humayun Kabir

Matric ID: T141007

Program: B. Sc. In ETE

Academic Year: Autumn 2017

## ACKNOWLEDGEMENT

### **In the name of Allah, the most Beneficent and most Merciful**

All praises and glory be to Allah (SWT) for blessing us with opportunities and showering upon us His mercy and guidance all through the life.

I express my gratitude, sincere appreciation and profound respect to my Supervisor **Engr. Syed Zahidur Rashid**, Assistant Professor of Electronic and Telecommunication Engineering, International Islamic University Chittagong, for his continuous guidance and advice in order to be successfully finishing the entire thesis work. While working, he has been a sincere mentor to do a quality research from the very beginning. He kept us focused on our thesis and helped us improve the quality of our thesis by giving invaluable feedback.

I would like to thank all faculty members, staff and fellow classmates of the Department of Electronic and Telecommunication Engineering, International Islamic University Chittagong, for their generous help in various ways for the completion of this thesis. I am also grateful to my parent and families for being extremely supportive while i was doing this work.

Author

Date:

Md. Humayun Kabir

## ABSTRACT

Nowadays, Energy Efficiency (EE) has become a buzzword for future wireless communication systems. Consequently, Massive Multiple Input and Multiple Output (MMIMO) technology have attained a great attention for Multi-User Communication scenario. MMIMO systems are crucial to maximizing energy efficiency (EE) and battery-saving technology. Achieving EE without sacrificing the quality of service (QoS) is increasingly important for mobile devices. We first derive the data rate through three linear precoding: Maximum Ratio Transmission (MRT), Zero-Forcing (ZF), and Minimum Mean Square Error (MMSE). Performance EE can be achieved when all available antennas are used and when taking account of the consumption circuit power ignored because of high transmit power. The aim of this work is to demonstrate how to obtain maximum EE while minimizing power consumed, which achieves a high data rate by deriving the optimal number of antennas and number of users in the massive MIMO system. The consumed power of the system includes transmitting power, circuit power consumption, and idle power consumption. The circuit power consumption dominates the system power consumption when the transmitter is equipped with the massive number of antennas. Hence, to analyze this problem, we propose a power consumption model. Maximized EE depends on the optimal number of antennas and determines the number of active users that should be scheduled in each cell. The results show the optimization of Energy with respect to the number of functioning mobile users, number of assigned base stations and launch input power in the system respectively.

## Table of Contents

Certificate of Approval .....	I
Declaration of Candidate .....	II
Acknowledgements .....	III
Abstract .....	IV
Table of Contents .....	V
List of Figure .....	IX
List of Table .....	X
List of Abbreviations .....	XI
List of Meaning of Symbols .....	XIII
<b>Chapter 01: Introduction</b>	<b>1 – 5</b>
1.1 Background of 5G .....	1
1.2 New technology in 5G .....	1
1.3 Expectations from 5G Cellular Networks .....	2
1.4 Need for Energy-Efficient Systems .....	3
1.5 Goal and Motivation .....	4
1.5.1 Goal .....	4
1.5.2 Motivation .....	4
1.6 Objectives .....	5
1.7 Thesis Outline .....	6
<b>Chapter 02: Literature Review</b>	<b>6 – 19</b>
2.1 Background on MIMO and Massive MIMO .....	6
2.2 Massive MIMO: A Multiuser MIMO Technology .....	6
2.2.1 Comparison between traditional MIMO and Massive MIMO ...	9
2.3 How Massive MIMO Works .....	9

2.3.1 Channel Estimation	9
2.3.2 Uplink Data Transmission	10
2.3.3 Downlink Data Transmission	10
2.4 Why Massive MIMO	10
2.5 Linear Signal Processing	11
2.6 Low-complexity User Scheduling	11
2.7 Precoding	12
2.8 Linear Precoding Schemes	13
2.8.1 Maximum-Ratio Combining (MRC) Detection	13
2.8.2 Zero-Forcing (ZF) Detection	13
2.8.3 Minimum Mean Squared Error (MMSE) Detection	14
2.9 Performance Comparison	14
2.10 Energy Efficiency in Massive MIMO	15
2.11 Methods to Improve Energy Efficiency in Massive MIMO Systems	16
2.11.1 Low-complexity BS operations	17
2.11.2 Minimize Power Amplifier (PA) Losses	18
2.11.3 Power Amplifier Dimensioning	18
2.11.4 Low PAPR Techniques	18
2.11.5 PA-Aware Design	19
2.12 Summary	19
<b>Chapter 03: Massive MIMO Cellular Systems Model</b>	<b>20 – 22</b>
3.1 System Models and Assumptions	20
3.2 Uplink Transmission	21
3.3 Downlink Transmission	21
3.4 Linear Processing	22

3.5 Linear Receivers (in the Uplink)	23
3.5.1 Maximum-Ratio Combining (MRC) Receiver	23
3.5.2 Zero-Forcing (ZF) Receiver	24
3.5.3 Minimum Mean-Square Error (MMSE) Receiver	24
3.6 Linear Precoders (in the Downlink)	25
3.7 Circuit Power Consumption Model	26
3.7.1 Transceiver Chains	27
3.7.2 Channel Estimation	27
3.7.3 Coding and Decoding	28
3.7.4 Backhaul	28
3.7.5 Linear Processing	28
3.8 Comparison of CP with Different Processing Schemes	29
3.9 Tradeoff between Power Consumption (PC) and Throughput	30
3.10 Problem Statement	31
3.10.1 Problem Solutions	32
<b>Chapter 04: Simulation and Result Analysis</b>	<b>33 – 45</b>
4.1 Why Simulation	33
4.2 Simulator	33
4.3 Implementation of the Model	33
4.4 Purpose of the Simulation	34
4.5 Simulation Parameters	34
4.6 Analysis of Simulation Result: Complex Multiplications	35
4.7 Analysis of Simulation Result: The Total CP	37
4.8 Analysis of Simulation Result: The Average SE	40
4.9 Analysis the Power Consumption and Throughput	41

4.10 Network Design for Maximal Energy Efficiency	.....	42
<b>Chapter 05: Conclusion and Future Work</b>		<b>46 – 47</b>
5.1 Conclusion	.....	46
5.2 Future Work	.....	47
<b>References</b>		<b>48</b>
<b>Appendix A</b>		<b>52</b>

## List of Figures

Figure 1.1: Total number of mobile phone users worldwide from 2013 to 2019	..... 1
Figure 1.2: Advancement in 5G	..... 2
Figure 1.3: Overview of services expected in future 5G networks	..... 2
Figure 1.4: Trends and forecast for greenhouse gas emissions.	..... 3
Figure 2.1: Massive MIMO: a multi-user MIMO technology	..... 7
Figure 2.2: Transmission protocol of TDD Massive MIMO	..... 9
Figure 2.3: Throughput comparison for different linear detection methods	..... 15
Figure 2.4: Overview of standard EE-maximization for massive MIMO systems	..... 17
Figure 3.1: Multiuser MIMO Systems	..... 20
Figure 3.2: Block diagram of linear detection at the BS	..... 22
Figure 3.3: Block diagram of the linear precoders at the BS	..... 26
Figure 4.1: Number of complex multiplications per cell when Fixed value of M	..... 35
Figure 4.2: Number of complex multiplications per cell when Fixed value of K	..... 36
Figure 4.3: Total CP vs. Number of Users (K) with fixed Antenna (M)	..... 38
Figure 4.4: Total CP vs. Number of Users (K) with fixed Users (K)	..... 38
Figure 4.5: Average DL and UL sum SE	..... 40
Figure 4.6: PC versus throughput for function of the different precoding schemes	... 41
Figure 4.7: Maximum Energy Efficiency per cell with MMSE Precoding Method	..... 43
Figure 4.8: Maximum Energy Efficiency per cell with ZF Precoding Method	..... 43
Figure 4.9: Maximum Energy Efficiency per cell with MRT Precoding Method	..... 43

## List of Tables

Table I: Computational Complexity for Different Receives Combining Schemes .....	30
Table II: Power Required for EachBSwith Different Combining Precoding Scheme...	30
Table III: Simulation Parameters .....	32
Table IV: Number of Complex Multiplications per cell when Fixed M .....	36
Table V: Number of Complex Multiplications per cell when Fixed K .....	37
Table VI: Comparison of Complex Multiplications per cell with Reference Paper .....	37
Table VII: Total CP per cell of both UL and DL for fixed user (K) .....	39
Table VII: Total CP per cell of both UL and DL for fixed antenna (M) .....	39
Table IX: Comparison of Total CP with Reference Paper .....	39
Table X: Comparison of Maximum EE with Reference Paper .....	44

## List of Abbreviations

5G	Fifth Generations
EE	Energy Efficiency
MMIMO	Massive Multiple Input and Multiple Output
ZF	Zero Forcing
MRT	Maximum Ratio Transmission
MMSE	Minimum Mean Square Error
D2D	Device to Device
ICT	Information and Communication Technology
LTE	Long Term Evolution
IoT	Internet of Things
Gbps	Giga bits per second
Mbps	Megabits per second
CP	Circuit Power
MIMO	Multiple-Input Multiple-Output
MU-MIMO	Multuser MIMO
UEs	User equipments
BS	Base station
SNRs	Signal to noise ratios
CSI	Channel State Information
ML	Maximum-likelihood
DPC	Dirty Paper Coding
RBF	Random Beamforming
SUS	Semi-orthogonal User Selection
CQI	Channel Quality Indicator

SINR	Signal to Interference plus Noise Ratio
SISO	Single-Input-to-Single-Output
PC	Power Consumption
SDMA	Space-Division Multiple Access
SE	Spectral Efficiency
TDD	Time-Division Duplex
PA	Power Amplifier
PAPR	Peak-to-average-power Ratio
OFDM	Orthogonal Frequency Division Multiplexing
FDD	Frequency-division Duplex
SIC	Successive Interference Cancellation
MSE	Mean Square Error
LO	Local Oscillator
ETP	Effective Transmit Power

## List of Meaning of Symbols

$M$	Number of Antenna
$K$	Number of Users
$C_{UL}$	Shannon capacities on the Uplink
$C_{DL}$	Shannon capacities on the Downlink
$\beta_k$	Large-scale Fading Coefficient
$p_u$	Average Signal to Noise Ratio
$I_M$	The $M \times M$ Identity Matrix
$\det(X)$	Determinant of a Square Matrix $X$
$H$	Channel Matrix
$g_k$	The $k^{\text{th}}$ Column of $H$
$H^*$	The Complex Conjugate of $H$
$H^T$	The Transpose of $H$
$H^H$	The Conjugate Transpose of $H$
$H^{-1}$	The Inverse of a Square Matrix $H$
$p_d$	The Average Transmission SNR
$C^{M \times K}$	The set of Complex-valued $M \times K$ Matrix
$z_k$	Additive Noise at the $k^{\text{th}}$ User
$D_q$	The Diagonal Matrix
$A$	Linear Detection Matrix
$P_{BS}$	Power per BS antennas for Transceiver Hardware
$P_{BT}$	Power per (bit/s) for Backhaul Traffic
$P_{COD}$	Power per (bit/s) for data encoding
$P_{DEC}$	Power per (bit/s) for data decoding
$P_{FIX}$	Fixed power of a BS

$P_{LO}$	Power per LO
$P_{UE}$	Power per UE for Transceiver Hardware
$P_{SYN}$	Power Consumed by the Local Oscillator
$P_{TC}$	Power Consumption by Transceiver Chains
$\tau_c$	Number of samples per Coherence Block
$\tau_d$	DL data samples per Coherence Block
$\tau_p$	Number of samples allocated for pilots per Coherence Block
$\tau_u$	UL data samples per Coherence Block
$B$	Total bandwidth used for Communication
$\bar{R}$	The User Gross Rates
$P_{TX}^{(ul)}$	UL Transmit Power per BS
$P_{TX}^{(dl)}$	DL Transmit Power per BS

# Chapter 01

## Introduction

This chapter presents an introduction to the thesis. An overview of Fifth Generation (5G) wireless system an Energy Efficiency (EE) perspective is given before a more detailed breakdown of the key aspects of the thesis.

### 1.1 Background of 5G

The rapid development of wireless communication technology has resulted in the explosive increases of mobile users. It has reported that there are over 1,069 million mobile users in Americas [2], while over 5 billion mobile phone users are projected to have on a global scale, which is shown in Fig. 1.1. The prevalence of smart devices leads to the explosive growth of requirements for digital wireless communication. As a result, the issue related to shortage of frequency resources is revealed. Although new technologies such as small cell and high order modulation can improve frequency efficiency to certain extent, it still cannot satisfy the requirements.

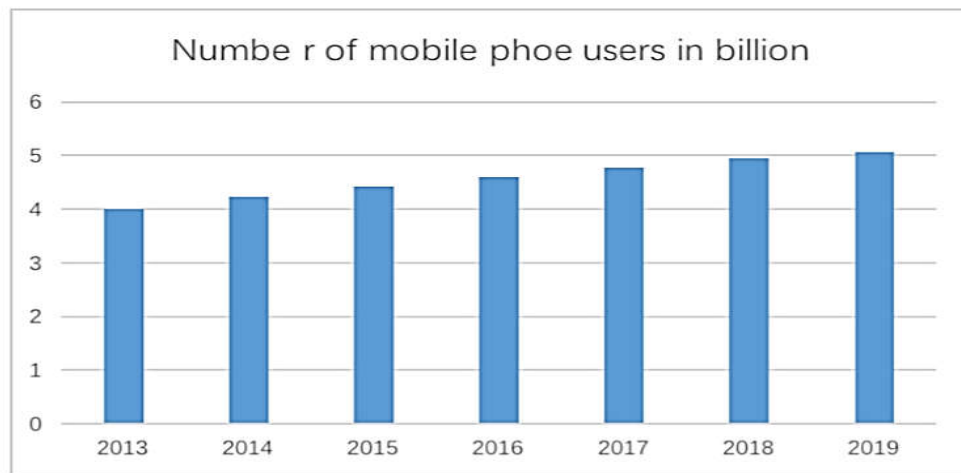


Figure 1.1: Total number of mobile phone users worldwide from 2013 to 2019 [1]

The fifth generation communication system (5G) is new emerging technology recent years since it enhances data speed, ultra reliable low latency, energy efficiency and massive machinetype communication [2]. Additionally, 5G wireless communication is not only for traditional mobile devices like smart phone and laptop, but also provides services for Device to Device (D2D) communications [2].

### 1.2 New technology in 5G

5G is expected to provide us with high capacity, low complexity, high data rate and ultra-

low latency communication system. The advancements in 5G are shown in Fig. 1.2 [2].

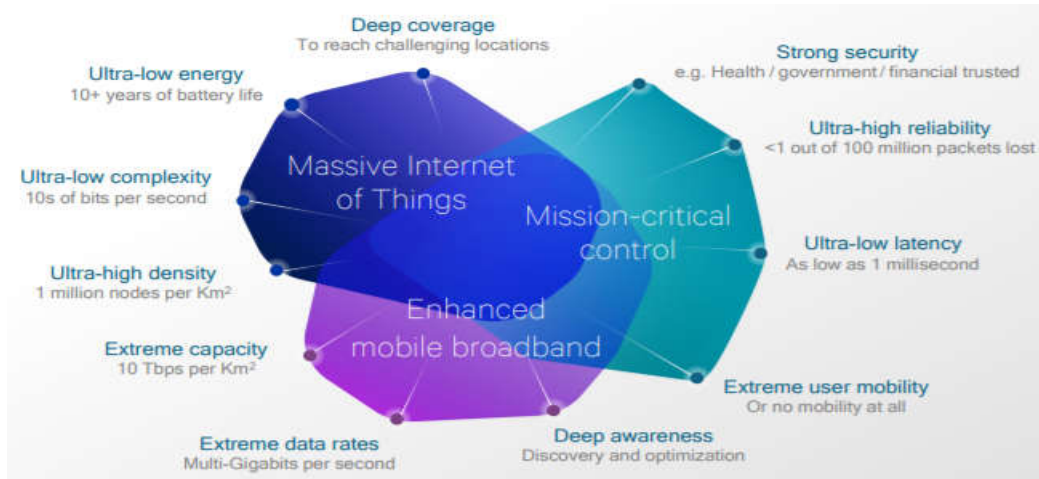


Figure 1.2: Advancement in 5G [2]

To achieve these goals, new technology including non-orthogonal multiple access, millimeter wave communication, massive MIMO, visible light communication, will be introduced. In this thesis, we will mainly focus on energy efficiency of massive MIMO systems [1, 2, and 3].

### 1.3 Expectations from 5G Cellular Networks

The information and communication technology (ICT) industry currently connects and manages billions of devices across the globe. Currently, we are in the era of 4G and 4.5G

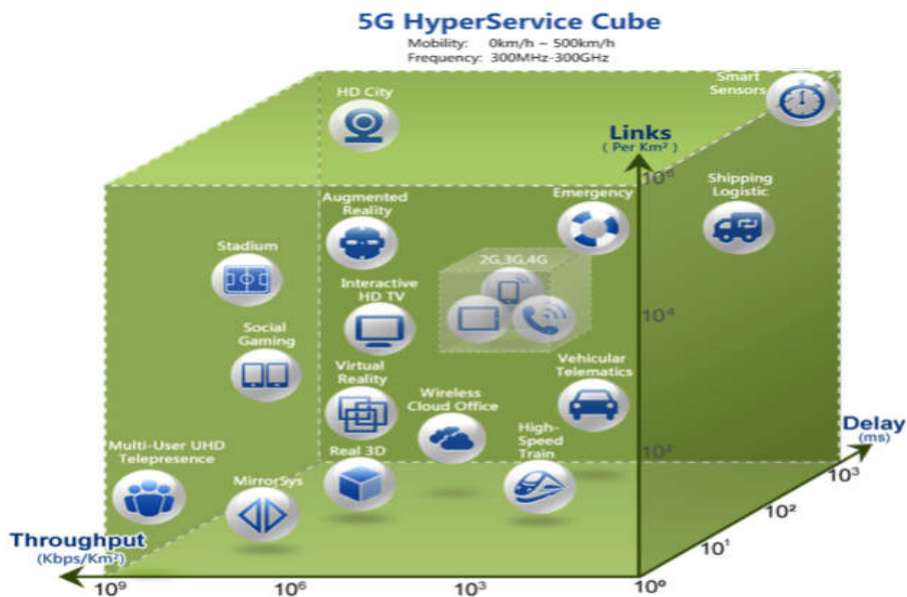


Figure 1.3: Overview of services expected in future 5G networks [2]

networks, which are referred to as Long Term Evolution (LTE) and LTE-Advanced networks respectively by standardization bodies. Global trends suggest that future 5G networks should handle up to a 1000-fold increase in the current traffic demands. In addition, a wide spectrum of services should be supported. See Figure 1.3 for an overview of 5G services envisioned by Huawei Technologies Co. Ltd. [5]. As we can observe from Fig. 1.3, the Internet of Things (IoT), which promises to connect almost everything, is expected to be an integral part of 5G networks. A host of emerging networks, such as, smart cities, vehicular networks, and augmented reality hubs will co-exist and operate simultaneously within 5G. In terms of technology demands, 5G networks should support latencies ranging from 1 millisecond (ms) to a few seconds, peak data rates up to 20 Giga bits per second (Gbps), average data rates up to 100 Megabits per second (Mbps), seamless connectivity for millions of IoT devices per square kilometer, and signaling loads ranging from 1% to almost 100% [5].

### 1.4 Need for Energy-Efficient Systems

When 5G networks are designed to meet such huge service expectations, energy consumption becomes a critical concern because mobile communication networks contribute towards a significant stake in the global carbon footprint.

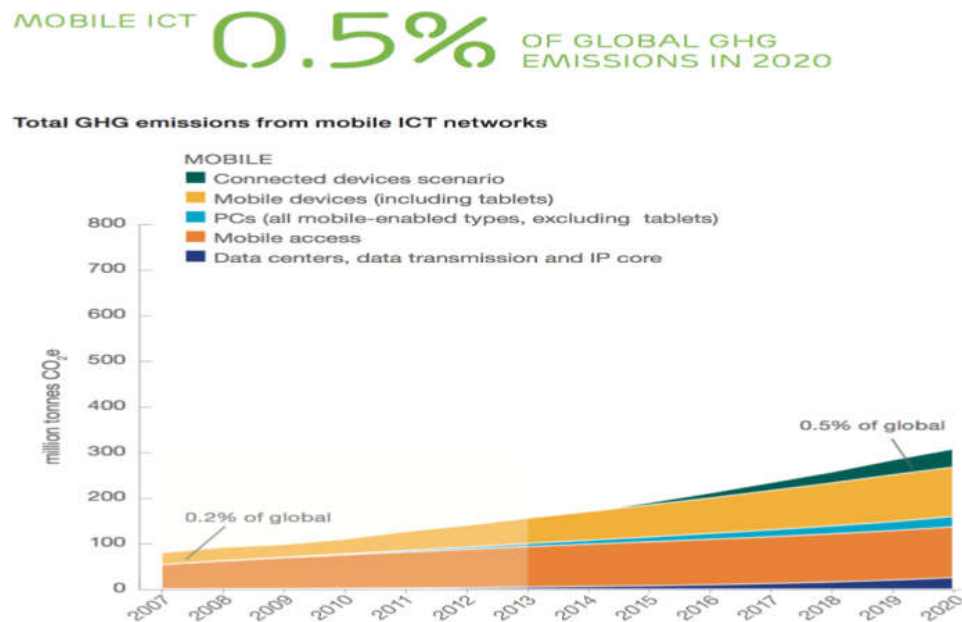


Figure 1.4: Trends and forecast for greenhouse gas emissions by the mobile ICT sector [2]

Trends [6] suggest that the mobile ICT sector would emit more than 300 million tonnes of greenhouse gases per annum by 2020. Observe from Figure 1.4 [4] that a majority of these emissions come from mobile access and mobile devices, i.e., from powering the wireless communications between the base stations (BSs) and the user equipment's

(UEs). Therefore, for a sustainable evolution into future 5G networks, it becomes critically important for future wireless technologies to not only address the multifold increase in service expectations, but also to operate at reduced power consumption levels. A key design parameter in this regard is the bit-per-joule energy efficiency, defined as:

$$\text{Energy Efficiency (bits/joule)} = \frac{\text{Throughput (bits/s)}}{\text{Power Consumption (Joule/s)}} \quad (1)$$

In equation (1), the energy efficiency (EE) of a wireless communication system can be increased by using methods which maximize the system throughput or minimize power consumption, or both. The focus of this thesis is on the massive multiple-input multiple-output (MIMO) technology, which offers higher EE levels current cellular communication networks.

## 1.5 Goal and Motivation

### 1.5.1 Goal

The goal of this thesis is to performance investigation of three precoding methods for maximal energy efficiency (EE) in the next-generation wireless communication system. Precoding methods such as Maximal Ratio Combining (MRC), Minimum mean square error (MMSE), and Zero-forcing (ZF). Our main goal is to find out which precoding method performs better based on the parameters like the number of an antenna (M), the number of users (K), throughput and power consumption.

### 1.5.2 Motivation

Massive MIMO is an emerging technology, which scales up the number of TX and RX antennas by at least an order of magnitude relative to conventional MU-MIMO systems. This approach leverages the spatial dimension providing significant increases in data rate, link reliability, energy efficiency, and multiplexing gains while reducing inter-user interference. Above the discussion this thesis will study energy efficiency in massive MIMO based on three pre-coding algorithms including MRC, MMSE and ZF in mathematical and simulation approaches. A simplified massive MIMO system is built in this system which equips with adjustable number of transmitted antenna and users with signal received antenna. In particular, a computational efficient resource allocation will be designed for the maximization of energy efficiency of the massive MIMO system. Besides, the impact of the amount of transmitted antenna on capacity will be assessed under different pre-coding algorithms. Based on this, energy efficiency will be then discussed. Finally, optimal and suboptimal transmission scheme will be presented in order to maximize the usage of materials and resources.

Based on this motivation, this thesis studies how massive MIMO technology can be used

to design maximum energy-efficient systems for future 5G deployments.

## 1.6 Objectives

The main purpose of the thesis is to provide insights on how  $M$ ,  $K$  and the transmit power affect the total EE of a multi-user massive MIMO system for different linear processing schemes at the BS. The objectives of this thesis are:

- a. To find the optimal number of base station antennas and users.
- b. To analyze the energy efficiency (EE) of Massive MIMO based on a Circuit Power (CP) consumption model.
- c. To analyze and achieve the optimal performance of maximize energy efficiency (EE) using different pre-coding algorithms.

## 1.7 Thesis Outline

This thesis is organized as follows:

Chapter 01: Introduction.

Chapter 02: Literature Review.

Chapter 03: Massive MIMO Cellular Systems Model.

Chapter 04: Simulation and Result Analysis.

Chapter 05: Conclusion and Future Work.

## Chapter 02

### Literature Review

To understand what massive MIMO is, as a new technology for wireless access, let us first overview the massive MIMO concept. This chapter describes the literature review of the thesis work, the theoretical advantages brought by scaling up MIMO, and the challenges we encounter in practice.

#### 2.1 Background on MIMO and Massive MIMO

One standard technique to increase throughput in a wireless communication system is to deploy multiple transceiver antennas at the transmitters and the receivers. When multiple antennas are used at the transmitters and the receivers, throughput gains can be achieved because the transmitter can spatially multiplex parallel streams of data over the same time frequency resource. Such multiple-input multiple-output (MIMO) systems have been under active research investigation over the last decade and are currently being used in LTE and LTE-Advanced networks.

Multiuser MIMO (MU-MIMO) systems [7], where a BS with multiple antennas can use scheduling algorithms to simultaneously serve multiple spatially-separated UEs over the same time-frequency resource have gained prominence because (i) MU-MIMO systems offer multiple access and broadcast capabilities and (ii) each UE in an MU-MIMO system can host a single antenna and still achieve similar throughput gains as achieved in point-to-point MIMO systems. In fact, the performance of point-to-point MIMO systems can be limited by the physical size and cost constraints at the UEs because the UEs are generally low-cost handheld devices and are therefore, unable to host several antennas.

**Definition 2.1:** Massive MIMO is a form of MU-MIMO systems where the number of BS antennas and the numbers of users are large. In Massive MIMO, hundreds or thousands of BS antennas simultaneously serve tens or hundreds of users in the same frequency resource.

#### 2.2 Massive MIMO: A Multiuser MIMO Technology

Massive MIMO is a multi-user MIMO technology in which  $K$  single-antenna user equipments (UEs) are serviced simultaneously on the same time-frequency resource by a base station (BS) equipped with a relatively large number  $M$  of antennas, i.e.,  $M \gg K$  (c.f. Fig. 2.1). In general, the UEs in a massive MIMO system can be equipped with more than one antenna. However, to simplify our analysis, discussions in this thesis are limited to systems with single-antenna UEs.

Deploying several antennas at the BS results in an interesting propagation scenario called favourable propagation, where the channel becomes near-deterministic because the radio links between the BS and the UEs become nearly orthogonal to each other [8]. This is because the effects of small-scale fading tend to disappear asymptotically in the large  $M$  regime. Significant EE gains can be achieved under favourable propagation because multiple orders of multiplexing and array gains are realizable. For the purpose of illustration, let us consider the uplink and downlink transmissions in a massive MIMO cell.

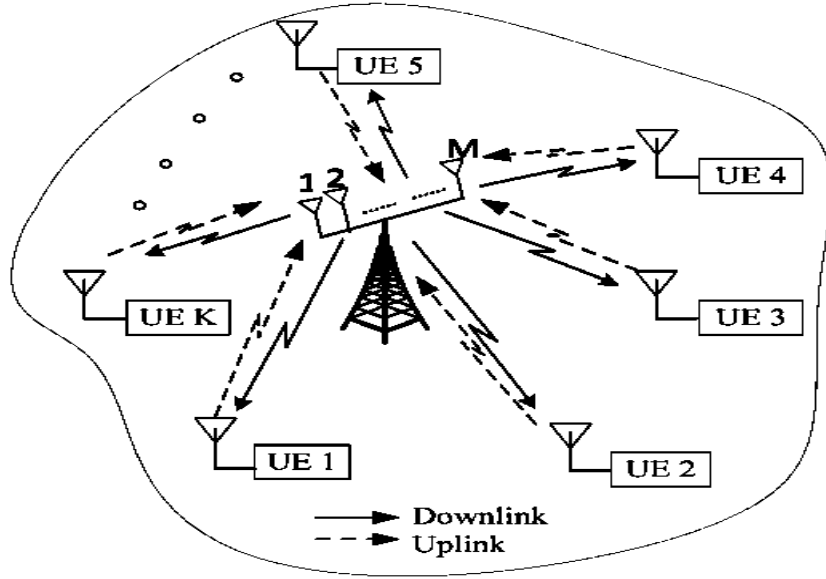


Figure 2.1: Massive MIMO: a multi-user MIMO technology where  $K$  single-antenna UEs are served by a BS with  $M \gg K$  antennas [8].

The asymptotic Shannon capacities on the uplink ( $C_{UL}$ ) and the downlink ( $C_{DL}$ ) for a multiuser MIMO channel under favourable propagation are given by [9]

$$C_{UL} = \sum_{k=1}^K \log_2(1 + p_{u,k} M \beta_k), \quad \text{----- (2.1)}$$

$$C_{DL} = \max_{(a_k \geq 0, \sum a_k \leq 1)} \sum_{k=1}^K \log_2(1 + p_{d,k} M a_k \beta_k)$$

Where  $p_{u,k}$  and  $p_{d,k}$  are the uplink and downlink signal to noise ratios (SNRs) for the  $k^{th}$  UE,  $\beta_k$  represents the large-scale fading coefficient for the  $k^{th}$  UE, and  $\{a_k, k=1, 2, \dots, K\}$ , is an optimization vector to obtain  $C_{DL}$ . For simplicity, if we neglect the

effect of  $\beta_k$  and assume that each UE transmits with an average signal to noise ratio  $p_u$ , the uplink Shannon capacity simplifies to

$$C_{UL} = K \log_2(1 + Mp_u) \quad \text{-----} \quad (2.2)$$

A similar argument can be made about downlink transmissions as well. The simplification illustrated in (2.2) leads us to two important observations (i) the system throughput can be improved by increasing  $K$ , i.e., by multiplexing parallel streams of data to more number of UEs over the same time-frequency resource, and (ii) transmission power per UE can be decreased by increasing  $M$ , i.e., the number of BS antennas, while still maintaining the same throughput per UE. In other words, the simplification in (2.2) shows that we can achieve  $O(K)$  multiplexing gains and  $O(M)$  array gains under favourable propagation.

While the large array gains are a straightforward opportunity to reduce UE transmission powers, massive MIMO also facilitates a drastic reduction in the circuit power consumed in the system. As discussed next, this is because the BS can implement (i) linear signal processing techniques and (ii) low-complexity user scheduling algorithms, and still achieves near-optimal throughput performance.

The main benefits of Massive MIMO systems are:

1. **Huge spectral efficiency and high communication reliability:** Massive MIMO inherits all gains from conventional MU-MIMO, i.e., with  $M$ -antenna BS and  $K$  single-antenna users, we can achieve a diversity of order  $M$  and a multiplexing gain of  $\min(M, K)$ . By increasing both  $M$  and  $K$ , we can obtain a huge spectral efficiency and very high communication reliability.
2. **High energy efficiency:** In the uplink Massive MIMO, coherent combining can achieve a very high array gain which allows for substantial reduction in the transmit power of each user. In the downlink, the BS can focus the energy into the spatial directions where the terminals are located. As a result, with massive antenna arrays, the radiated power can be reduced by an order of magnitude, or more, and hence, we can obtain high energy efficiency. For a fixed number of users, by doubling the number of BS antennas, while reducing the transmit power by two, we can maintain the original the spectral efficiency, and hence, the radiated energy efficiency is doubled.
3. **Simple signal processing:** For most propagation environments, the use of an excessive number of BS antennas over the number of users yields favorable propagation where the channel vectors between the users and the BS are pairwise (nearly) orthogonal. Under favorable propagation, the effect of interuser interference and noise can be eliminated with simple linear signal processing (linear precoding in the downlink and linear decoding in the uplink). As a result,

simple linear processing schemes are nearly optimal. Another key property of Massive MIMO is channel hardening. Under some conditions, when the number of BS antennas is large, the channel becomes deterministic, and hence, the effect of small-scale fading is averaged out. The system scheduling, power control, etc., can be done over the large-scale fading time scale instead of over the small-scale fading time scale. This simplifies the signal processing significantly.

**2.2.1 Comparison between traditional MIMO and Massive MIMO**

Compared to traditional MIMO, the advantages of massive MIMO include [2-5]:

- Enhancement of SE
- Massive amount of degrees of freedom in spatial domain
- Good system performance with only linear precoding scheme, e.g. Zero forcing, Maximum Ratio Transmission, Minimum Mean Square Error
- Facilitate resource allocation

**2.3 How Massive MIMO Works**

In Massive MIMO, TDD operation is preferable. During a coherence interval, there are three operations: channel estimation (including the uplink training and the downlink training), uplink data transmission, and downlink data transmission. A TDD Massive MIMO protocol is shown in Figure 2.2.

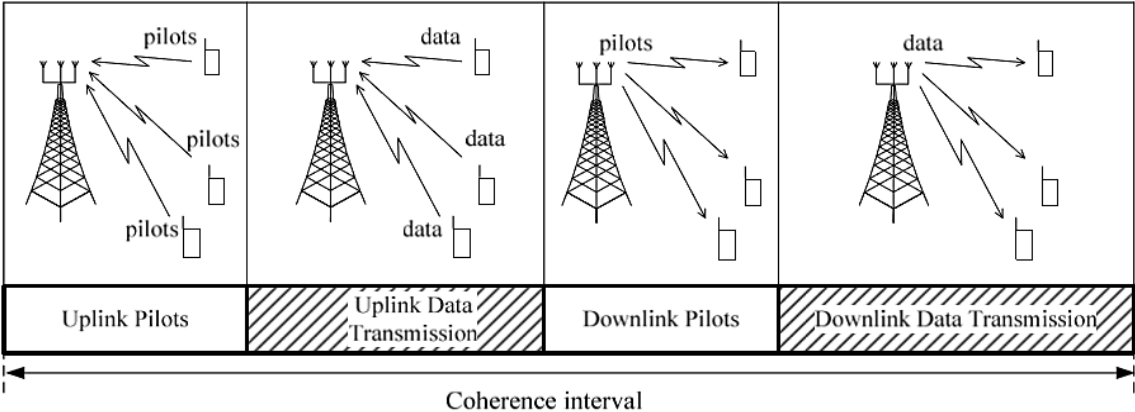


Figure 2.2: Transmission protocol of TDD Massive MIMO [10].

**2.3.1 Channel Estimation**

The BS needs CSI to detect the signals transmitted from the users in the uplink, and to precode the signals in the downlink. This CSI is obtained through the uplink training. Each user is assigned an orthogonal pilot sequence, and sends this pilot sequence to the BS. The BS knows the pilots sequences transmitted from all users, and then estimates the channels based the received pilot signals.

Furthermore, each user may need partial knowledge of CSI to coherently detect the signals transmitted from the BS. This information can be acquired through downlink training or some blind channel estimation algorithm. Since the BS uses linear precoding techniques to beamform the signals to the users, the user needs only the effective channel gain to detect its desired signals. Therefore, the BS can spend a short time to beamform pilots in the downlink for CSI acquisition at the users [10].

### 2.3.2 Uplink Data Transmission

A part of the coherence interval is used for the uplink data transmission. In the uplink, all K users transmit their data to the BS in the same time-frequency resource [11]. The BS then uses the channel estimates together with the linear combining techniques to detect signals transmitted from all users. The detailed uplink data transmission was discussed in detail in later Section.

### 2.3.3 Downlink Data Transmission

In the downlink, the BS transmits signals to all K users in the same time-frequency resource [12]. More specially, the BS uses its channel estimates in combination with the symbols intended for the K users to create M precoded signals which are then fed to M antennas. The downlink data transmission was discussed in detail in later Section.

## 2.4 Why Massive MIMO

The demand for wireless throughput and communication reliability as well as the user density will always increase. Future wireless communication requires new technologies in which many users can be simultaneously served with very high throughput. Massive MIMO can meet these demands. Consider the uplink transmission. The same argument can be used for the downlink transmission. From (2.2), the sum-capacity of the uplink transmission is [10]:

$$C_{sum} = \log_2 \det(I_K + p_u M I_K) = K \log_2(1 + p_u M) \dots \dots \dots (2.3)$$

In (2.3), K is the multiplexing gain, and M represents the array gain. We can see that, we can obtain a huge spectral efficiency and energy efficiency when M and K are large. Without any increase in transmitted power per terminal, by increasing K and M, we can simultaneously serve more users in the same frequency band. At the same time the throughput per user also increases. Furthermore, by doubling the number of BS antennas, we can reduce the transmit power by 3 dB, while maintaining the original quality-of-service.

The above gains are obtained under the conditions of favorable propagation and the use of optimal processing at the BS. In Massive MIMO, when the number of BS antennas is

large, due to the law of large numbers, the channels become favorable. As a result, linear processing is nearly optimal. The multiplexing gain and array gain can be obtained with simple linear processing. Also, by increasing the number of BS antennas and the number of users, we can always increase the throughput.

## 2.5 Linear Signal Processing

In conventional multiuser MIMO systems, optimal capacities can be achieved if the BS implements complex signal processing techniques, such as, maximum-likelihood (ML) multiuser detection on the uplink and dirty paper coding (DPC) [6] on the downlink. Unfortunately, such complex signal processing techniques incur large computational burdens which grow exponentially with the size of the system, for example with the number of BS antennas  $M$ . As a result, when  $M$  and  $K$  are large, such techniques consume large amounts of circuit power, thus becoming highly unsuitable for massive MIMO operations.

Fortunately, in the large  $M$  regime, linear signal processing techniques, such as maximum-ratio combining (MRC) on the uplink and maximum-ratio transmission (MRT) on the downlink, can achieve near-optimal throughput performance.

## 2.6 Low-complexity User Scheduling

In conventional multiuser MIMO systems, simple linear precoding techniques, such as maximum ratio transmission (MRT), do not achieve optimal capacities on the downlink. To reduce the performance gap, the BSs generally implement certain user scheduling methods which exploit multi-user diversity in the system. Basically, the BS selects few UEs during each transmission interval and schedules them for simultaneous transmissions. Two seminal works on user scheduling are the random beamforming (RBF) and the semi-orthogonal user selection (SUS) [8] methods. In the RBF method, the BS selects a group of UEs by matching them to a pre-determined set of orthogonal beams transmitted on the downlink. The matching is based on feedback provided by each UE, in terms of a channel quality indicator (CQI), such as the signal to interference plus noise ratio (SINR), and the best beam index. In SUS method, the BS acquires full channel state information (CSI) from the entire candidate UEs and selects a subset of UEs which have near-orthogonal channel vectors.

Conventional user scheduling methods, such as RBF or SUS, may not be appropriate for massive MIMO systems due to a variety of reasons: (i) performance gains based on multiuser diversity may not be significant in the large  $M$  regime because the effects of small scale fading are diminished (ii) such methods are computationally intensive and consume significant amounts of circuit power when  $M$  is large – SUS incurs  $O(M^3K)$  computational complexity [8], and (iii) such methods often suffer from practical

limitations—RBF schemes do not perform well in systems with finite number of UEs [13] and SUS schemes are unsalable because significant overhead is incurred when acquiring full CSI from all the candidate UEs.

Fortunately, in the large  $M$  regime, very simple user scheduling schemes, such as, selecting a subset of UEs randomly [15], selecting a subset of UEs in the descending order of their large-scale fading coefficients [15], or selecting UEs in a round-robin fashion [16], are known to achieve near-optimal throughput performance. This is because the channel vectors become near-orthogonal to each other and the effects of small-scale fading are diminished in the large  $M$  regime.

Since low-complexity signal processing and user scheduling algorithms achieve near optimal throughput performance in massive MIMO systems, we observe that the circuit power consumption is drastically reduced when compared to conventional multiuser MIMO systems. Note that this reduction in circuit power consumption is in addition to the large array gains, which allow for a significant reduction in the UE transmission powers. Consequently, by achieving near-optimal throughput performance at reduced power consumption levels, massive MIMO networks deliver multiple orders of EE gains over current LTE networks.

In the next section, we present a discussion on three prominent linear multiuser detection techniques for massive MIMO, namely maximum-ratio combining (MRC), zero-forcing (ZF) detection, and minimum mean squared error (MMSE) detection. We explain how these linear detection techniques are derived and show that these techniques achieve near-optimal throughput performance in the large  $M$  regime.

## 2.7 Precoding

Precoding provides two fundamental advantages, including eliminate interference and performing beamforming to the desired users. In general, there are two types of precoding, non-linear precoding schemes and linear pre-coding schemes. Non-linear precoding can achieve both of these two functions, while the linear one can only reduce inter-users interference [18].

In wireless communication system, due to the geographic effect, received signal cannot be obtained simultaneously [19]. Inter-user interference cannot be eliminated by multi-user detection as well. Under this circumstance, precoding will play a significant role in improving system performance.

Compared to nonlinear precoding schemes, the complexity of linear precoding schemes the complexity is remarkably lower. Moreover, due to a massive amount of degrees of

freedom in massive MIMO, linear precoding schemes are enough to satisfy communication requirements [17, 19].

## 2.8 Linear Precoding Schemes

In massive MIMO systems, when the amount of transmitted antennas approaches infinity, the system can be simplified as Single-input-to-Single-output (SISO) systems [20]. Therefore, to optimize spectral resources in massive MIMO systems, pre-coding is used at the transmit side in order to reduce the complexity of system, diminish noise effect and optimize stream data transmission based on channel state information (CSI) [21,22,23]. There are three common linear pre-coding schemes, including MRC, ZF and MMSE.

### 2.8.1 Maximum-Ratio Combining (MRC) Detection

This scheme is to maximize SNR by seeking to maximize the power at the receiver combiner. MRC is considered as a viable linear reception scheme for massive MIMO systems since it can be applied in a distributed manner. The mathematical model for MRC is shown as below,

$$W = \frac{g_k}{\|g_k\|} = H \dots\dots\dots (2.4)$$

Moreover, MRC has a satisfactory performance in the low-power regime, even approaching to optimal performance as the amount of antennas grows infinitely. However, as the power increase, systems based on MRC scheme suffer from serious inter-user interference [16].

**Advantage:** The signal processing is very simple since the BS just multiplies the received vector with the conjugate-transpose of the channel matrix  $H$ , and then detects each stream separately. More importantly, MRC can be implemented in a distributed manner. This implies that at low SNR, MRC can achieve the same array gain as in the case of a single-user system.

**Disadvantage:** As discussed above, since MRC neglects the effect of multiuser interference, it performs poorly in interference-limited scenarios.

### 2.8.2 Zero-forcing (ZF) Detection

The ZF scheme is to eliminate inter-user interference by projecting the received signals into the orthogonal elements. It can be written as

$$W = H (H^H H)^{-1} \dots\dots\dots (2.5)$$

Since ZF scheme does not take noise into consideration, system based on ZF precoding scheme has a poor performance in low power regime. The performance in high-power regime approaches to optimal [16].

**Advantage:** The signal processing is simple and ZF works well in interference-limited scenarios. The SINR can be made as high as desired by increasing the transmit power.

**Disadvantage:** Since ZF neglects the effect of noise, it works poorly under noise-limited scenarios. Furthermore, if the channel is not well conditioned then the pseudo-inverse amplifies the noise significantly, and hence, the performance is very poor. Compared with MRC, ZF has a higher implementation complexity due to the computation of the pseudoinverse of the channel gain matrix.

### 2.8.3 Minimum Mean Squared Error (MMSE) Detection

MMSE scheme seeks to eliminate inter-user interference as well as noise. Compared to MRC and ZF, system complexity of MMSE is relatively higher.

$$W = H \left( H^H H + \frac{1}{p_u} I_M \right)^{-1} \dots\dots\dots (2.6)$$

From mathematical perspective, MRC has the lowest complexity among these three precoding schemes. MMSE requires perfect channel state information [16].

## 2.9 Performance Comparison

Figure 2.3 plots the throughput performance of MRC, ZF, and MMSE detection methods when the number of BS antennas is increased up to 100. We assume  $K = 10$ ,  $p_u = -10$  dB, and calculate the uplink sum-rates, where values are calculated for the three detectors by substituting the detection matrices in (2.4), (2.5) and (2.6). When  $M$  is large, we observe that all the linear detection methods achieve near-optimal throughput performance. The MRC detection method does not perform as well as the other two linear detection methods because it neglects the effects of inter-user interference in the system.

Nevertheless, the performance of MRC is comparable to the other two methods and is, in fact, the preferred choice for practical deployments because (i) MRC requires minimal number of computations and hence incurs low circuit power consumption and (ii) MRC does not suffer from noise amplification when the channels are ill-conditioned, as often experienced in practice.

On similar lines to our discussions for linear multiuser detection methods, linear precoders can also be derived for downlink transmissions in a massive MIMO system. Three prominent linear precoders in the current literature, namely maximum-ratio

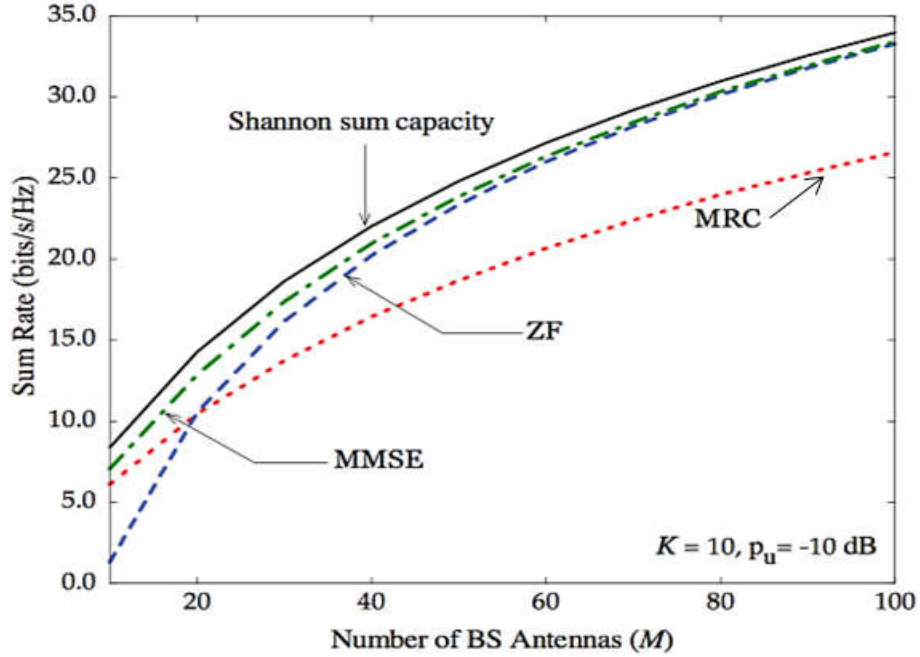


Figure 2.3: Throughput comparison for different linear detection methods respect to number of antenna (M) [8].

transmission (MRT), zero-forcing (ZF), and minimum mean squared error (MMSE) precoders, have similar operational meanings and exhibit similar properties as MRC, ZF, and MMSE detection techniques respectively. Therefore, the precoding matrices  $W^{MRC}$ ,  $W^{ZF}$  and  $W^{MMSE}$  for the three linear precoders mentioned above are given by

$$\begin{aligned}
 W^{MRC} &= H, \\
 W^{ZF} &= H(H^H H)^{-1} \\
 W^{MMSE} &= \left( H^H H + \frac{1}{p_d} I_M \right)^{-1} \dots \dots \dots (2.7)
 \end{aligned}$$

Where  $p_d$  is the average transmission SNR on the downlink. Similar to the case with lineardetection methods, these linear precoders achieve near-optimal throughput performance in the large M regime. This completes our discussion on how signal processing requirements are simplified in massive MIMO systems.

The next section presents a few guidelines on how realistic power consumption models can be developed for massive MIMO systems. This is important because the EE metric, relies on the accuracy of power consumption model used.

## 2.10 Energy Efficiency in Massive MIMO

In massive MIMO system, when allocating transmitted power equally to antennas, the spatialefficiency will be improved by M and  $\sqrt{M}$  for perfect CSI and imperfect CSI

system, respectively where M represents the number of transmitted antennas. Moreover, with the increase amount of antennas, noise and small scale fading will decrease correspondingly; correlation among channels will be reduced by expending distance among antennas. According to statistics, channels between antennas and users will approach to orthogonal when the number of antennas is overwhelmingly large than that of users [18]. Traditional MIMO systems pay more attention on transmitted power consumption instead of EE [20].

Massive MIMO aims at evolving the coverage tier BSs by using arrays with a hundred or more antennas, each transmitting with a relatively low power. This allows for coherent multiuser MIMO transmission with tens of UEs being spatially multiplexed in both UL and DL of each cell. The area throughput is improved by the multiplexing gain. However, the throughput gains provided by Massive MIMO come from deploying more hardware (i.e., multiple RF chains per BS) and digital signal processing (i.e., SDMA combining/precoding) which, in turn, increase the CP per BS [28].

EE refers to how much energy it takes to achieve a certain amount of work. This general definition applies to all fields of science, from physics to economics, and wireless communication is no exception [24]. Unlike many fields wherein the definition of “work” is straightforward, in a cellular network it is not easy to define what exactly one unit of “work” is. The network provides connectivity over a certain area and it transports bits to and from UEs. Users pay not only for the delivered number of bits but also for the possibility to use the network anywhere at any time. Moreover, grading the performance of a cellular network is more challenging than it first appears, because the performance can be measured in a variety of different ways and each such performance measure affects the EE metric differently. Among the different ways to define the EE of a cellular network, one of the most popular definitions takes inspiration from the definition of SE, that is, “the SE of a wireless communication system is the number of bits that can be reliably transmitted per complex-valued sample. By replacing “SE” with “EE” and “complex-valued sample” with “unit of energy”, the following definition is obtained [24, 25, 28]:

**Definition 5.1:** The Energy efficiency (EE) of a cellular network is the number of bits that can be reliably transmitted per unit of energy.

$$\text{Energy Efficiency (EE)} = \frac{\text{Throughput (bit/s/cell)}}{\text{Power Consumption (W/cell)}} \dots\dots\dots (2.8)$$

which is measured in bit/Joule and can be seen as a benefit-cost ratio, where the service quality (throughput) is compared with the associated costs (power consumption).

## 2.11 Methods to Improve Energy Efficiency in Massive MIMO Systems

Observe, from (2.8), that the energy efficiency of a massive MIMO network can be maximized by achieving optimal throughput performance while operating at minimum levels of power consumption. Based on this analogy, a number of research directions have been pursued for the design of energy-efficient massive MIMO networks see Fig 3.1 for a broad overview. Few methods devise low-complexity algorithms for BS operations, such as, multi-user detection, precoding, and user scheduling, so as to achieve near-optimal throughput performance at low power expenditure. Few other methods, such as, transceiver re-design, antenna selection, and power amplifier dimensioning, focus on improving resource utilization in the system so as to relax hardware requirements and thereby, the power expenditure in the system. Available literature also includes methods which minimize power losses in the system, such as, antenna reservation and amplifier-aware design, and methods which relax hardware quality, i.e., by introducing hardware imperfections, to reduce power expenditure in the system. In this section, we study some of the techniques mentioned above and identify few open research challenges thereof.

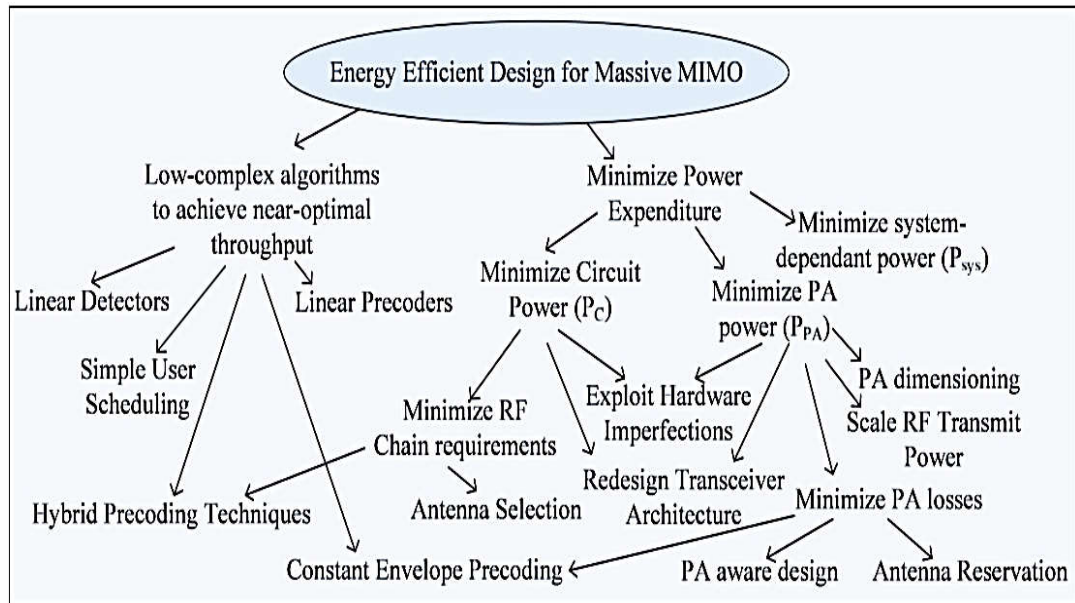


Figure 2.4: Overview of standard EE-maximization techniques for massive MIMO systems [8].

### 2.11.1 Low-complexity BS operations

Due to favourable propagation in the large  $M$  regime, simple linear processing techniques, such as Maximum-Ratio Combining (MRC) and Maximum-Ratio Transmission (MRT) precoding, and simple user scheduling algorithms, such as random and round robin scheduling, achieve near-optimal throughput performance. These simplifications yield significant EE gains because the circuit power  $P_C$  is drastically

reduced when compared to conventional systems with computationally intensive signal processing schemes, such as ML detection and successive interference cancellation (SIC), and complex scheduling algorithms, such as random beamforming and semi-orthogonal user selection.

While channel reciprocity can be exploited in TDD systems to derive near-optimal low complexity linear precoding schemes, precoders for FDD systems cannot exploit channel reciprocity because the UL and DL communications occur on separate frequency bands. FDD precoders cannot also rely on pilot signalling and feedback from the UEs because this consumes at least  $M + K$  symbols per coherence interval, making them impractical for high mobility scenarios. Few low overhead FDD precoders, which assume channel sparsity for channel dimensionality reduction, have been proposed recently [26]. However, such precoders are limited to high frequency bands, such as mmWave, where channel sparsity assumptions are valid. Consequently, low-complexity and low-overhead FDD precoding continues to be a major research challenge for massive MIMO networks. Since there are many more licenses worldwide for FDD than for TDD, progress on low overhead FDD precoders will promotewider acceptance of massive MIMO as a future technology.

### **2.11.2 Minimize Power Amplifier (PA) Losses**

Significant energy efficiency gains can be achieved by minimizing power amplifier losses because inefficient power amplifier operations in the current LTE networks discard as much as 60% to 95% of the power input to the amplifiers [27]. Prominent research directions to minimize power amplifier losses include (i) dimensioning the power amplifier, (ii) use of low peak-to-average-power-ratio (PAPR) techniques, and (iii) PA-aware design.

### **2.11.3 Power Amplifier Dimensioning**

Losses at the power amplifiers can be minimized by operating the power amplifiers at points close to the maximum allowed output. Unfortunately, most power amplifiers in current LTE deployments are operated, on an average, at points much lower than the maximum allowed output because of the high linearity requirements imposed by high peak to average power (PAPR) waveforms such as OFDM. Power losses at linear power amplifiers can be reduced significantly by adaptively dimensioning, i.e., adjusting, the power amplifier's maximum output power based on temporal variations in the traffic load in the system. Such load adaptive power amplifier dimensioning techniques are known to enhance the energy efficiency of massive MIMO systems by up to 30 % [8]. A major drawback for power amplifier dimensioning methods is that their performance is sensitive to the accuracy of available information on temporal traffic variations in the system, which are generally very difficult to predict.

### 2.11.4 Low PAPR Techniques

As an alternative to linear power amplifiers, the BS can deploy non-linear power amplifiers, which are known to be about 4-6 % more power efficient [26]. However, non-linear PAs require low PAPR input signals to avoid signal distortions. To address this concern, researchers have been exploring different PAPR reduction methods. For example, few antenna reservation methods have been recently proposed [24], wherein the signals sent to one set of antennas are deliberately clipped so as to achieve low PAPR, while correction signals are sent on the remaining set of reserved antennas so as to compensate for the clipping. In [8], the authors assume  $M = 100$  and reserve 25 % of the antennas so as to achieve a PAPR reduction of 4 dB. A major drawback with antenna reservation methods is that they may not necessarily increase the system energy efficiency because reserving antennas results in reduced throughput and the reservation process increases signaling overhead in the system.

Few low-PAPR non-orthogonal waveforms, such as single carrier modulation (SCM), have been proposed recently. However, designing appropriate non-orthogonal waveforms continues to be a major research challenge because most of the recently proposed non-orthogonal waveforms suffer from limitations, such as long filter lengths and complex receiver techniques. Linearity requirements of power amplifiers can also be relaxed using constant envelope input signals. When appropriate precoding schemes are employed, constant envelope signals can achieve similar throughputs as achieved by high-PAPR signals. A major unresolved challenge concerning constant envelope signal studies is the generation of perfectly constant envelope continuous-time signals.

### 2.11.5 PA-Aware Design

A different approach to minimize power amplifier losses is the design of PA-aware massive MIMO systems. This can be beneficial because conventional massive MIMO systems, designed with sum-power constraints per BS, do not impose constraints on the maximum output power and the power loss per PA. Recent studies on simple MIMO systems [8] show that significant improvements in the throughput performance per UE can be achieved when PA-aware design is implemented with realistic constraints on both the PA output power and the power losses per PA. We observe that the design of PA-aware systems is a relatively new research field with no literature currently available for massive MIMO systems.

## 2.12 Summary

In this chapter, we discuss massive MIMO technology. By analyzing system capacity and power consumption, we obtain that the energy efficiency is closely associated to the transmitted power and the number of activated antennas.

## Chapter 03

### Massive MIMO Cellular Systems Model

In the previous chapter, the basic theory of massive MIMO system has been discussed. In massive MIMO systems, since a large amount of antennas arrays are implemented, we can achieve a desired capacity with lower power consumption. In this chapter, we will concentrate on the achievable capacity of massive MIMO systems. In theory, the base station will apply the maximum likelihood detector in order to achieve optimal capacity. Under this circumstance, however, the complexity in received side will be exponentially raised as increase of the number of users. As we discussed previously, in massive MIMO systems, linear coding schemes can also meet our requirements. Therefore, in this chapter, we will theoretically analyze the system performance of massive MIMO based on ZF, MRC and MMSE.

#### 3.1 System Models and Assumptions

Massive MIMO is a MU-MIMO cellular system where the number of BS antennas and the number users are large. We consider a MU-MIMO system which consists of one BS and  $K$  active users. The BS is equipped with  $M$  antennas, while each user has a single-antenna. In general, each user can be equipped with multiple antennas. However, for simplicity of the analysis, we limit ourselves to systems with single-antenna users. See Figure 3.1. We assume that all  $K$  users share the same time-frequency resource. Furthermore, we assume that the BS and the users have perfect CSI. The channels are acquired at the BS and the users during the training phase. The specific training schemes depend on the system protocols frequency-division duplex (FDD) or time-division duplex (TDD), and will be discussed in detail in Section 2.5.

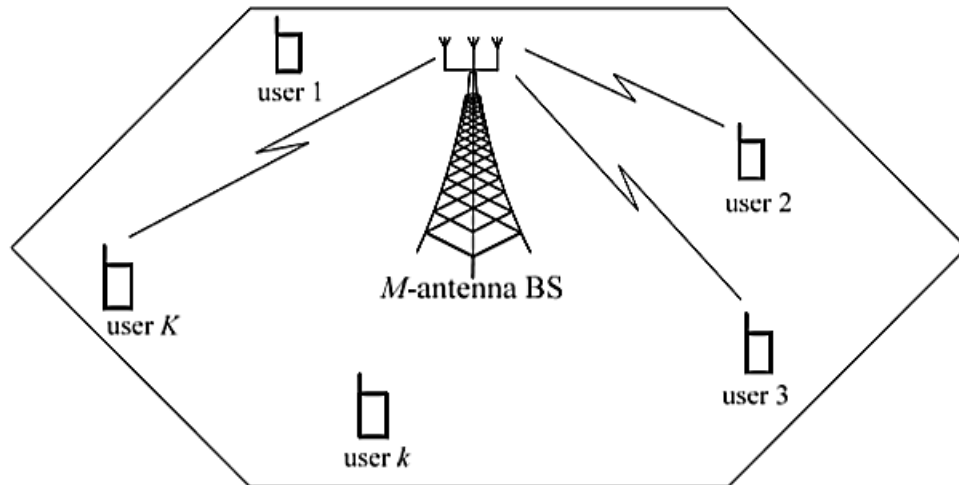


Figure 3.1: Multiuser MIMO Systems. Here,  $K$  single-antenna users are served by the  $M$ -antenna BS in the same time-frequency resource [12].

Let  $H \in \mathbb{C}^{M \times K}$  be the channel matrix between the  $K$  users and the BS antenna array, where the  $k^{th}$  column of  $H$ , denoted by  $h_k$ , represents the  $M \times 1$  channel vector between the  $k^{th}$  user and the BS. In general, the propagation channel is modeled via large-scale fading and small-scale fading. But in this chapter, we ignore large-scale fading, and further assume that the elements of  $H$  are i.i.d. Gaussian distributed with zero mean and unit variance.

### 3.2 Uplink Transmission

Uplink (or reverse link) transmission is the scenario where the  $K$  users transmit signals to the BS. Let  $s_k$ , where  $\mathbb{E}\{\|s_k\|^2\} = 1$ , be the signal transmitted from the  $k^{th}$  user. Since  $K$  users share the same time-frequency resource, the  $M \times 1$  received signal vector at the BS is the combination of all signals transmitted from all  $K$  users [10]:

$$y_{ul} = \sqrt{p_u} \sum_{k=1}^K h_k s_k + n \dots \dots \dots (3.1)$$

$$= \sqrt{p_u} H s + n \dots \dots \dots (3.2)$$

Where  $p_u$  is the average signal-to-noise ratio (SNR),  $n \in \mathbb{C}^{M \times 1}$  is the additive noise vector, and  $s \triangleq [s_1 \dots \dots \dots s_K]^T$ . We assume that the elements of  $n$  are i.i.d. Gaussian random variables (RVs) with zero mean and unit variance, and independent of  $H$ .

From the received signal vector  $y_{ul}$  together with knowledge of the CSI, the BS will coherently detect the signals transmitted from the  $K$  users. The channel model (3.2) is the multiple-access channel which has the sum-capacity [29].

$$C_{ul,sum} = \log_2 \det(I_K + p_u H^H H) \dots \dots \dots (3.3)$$

The aforementioned sum-capacity can be achieved by using the successive interference cancellation (SIC) technique [10]. With SIC, after one user is detected, its signal is subtracted from the received signal before the next user is detected.

### 3.3 Downlink Transmission

Downlink (or forward link) is the scenario where the BS transmits signals to all  $K$  users. Let  $x \in \mathbb{C}^{M \times 1}$ , where  $\mathbb{E}\{\|x\|^2\} = 1$ , be the signal vector transmitted from the BS antenna array. Then, the received signal at the  $k^{th}$  user is given by [10]:

$$y_{dl,k} = \sqrt{p_d} h_k^T x + z_k \dots \dots \dots (3.4)$$

Where  $p_d$  the average SNR and  $z_k$  is the additive noise at the  $k^{th}$  user. We assume that  $z_k$  is Gaussian distributed with zero mean and unit variance. Collectively, the received signal vector of the  $K$  users can be written as

$$y_{dl} = \sqrt{p_d} H^T x + z \dots \dots \dots (3.5)$$

Where  $y_{dl} \triangleq [y_{dl,1} y_{dl,2} \dots \dots y_{dl,K}]^T$  and  $z \triangleq [z_1 z_2 \dots \dots z_K]^T$ . The channel model (3.5) is the broadcast channel whose sum-capacity is known to be

$$C_{sum} = \max_{q_k \geq 0, \sum_{k=1}^K q_k \leq 1} \log_2 \det(I_M + p_u H^* D_q H^T) \dots \dots \dots (3.6)$$

Where  $D_q$  is the diagonal matrix whose  $k^{th}$  diagonal element is  $q_k$ . The sum-capacity (3.6) can be achieved by using the dirty-paper coding (DPC) technique.

### 3.4 Linear Processing

To obtain optimal performance, complex signal processing techniques must be implemented. For example, in the uplink, the maximum-likelihood (ML) multiuser detection can be used. With ML multiuser detection, the BS has to search all possible transmitted signal vectors  $\mathbf{s}$ , and choose the best one as follows:

$$\hat{\mathbf{s}} = \arg \max_{\mathbf{s} \in \mathcal{S}^K} \|\mathbf{y}_{ul} - \sqrt{p_u} H \mathbf{s}\|^2 \dots \dots \dots (3.7)$$

Where  $\mathcal{S}$  is the finite alphabet of  $\mathbf{s}_k, k = 1, 2, \dots, K$ . The problem (3.7) is a least squares (LS) problem with a finite-alphabet constraint. The BS has to search over  $|\mathcal{S}|^K$  vectors, where  $|\mathcal{S}|$  denotes the cardinality of the set  $\mathcal{S}$ . Therefore, ML has a complexity which is exponential in the number of users.

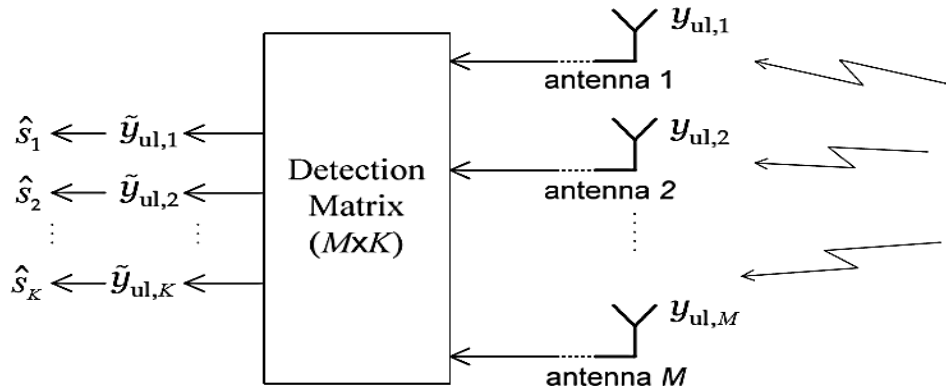


Figure 3.2: Block diagram of linear detection at the BS [12].

The BS can use linear processing schemes linear receivers in the uplink and linear precoders in the downlink to reduce the signal processing complexity. These schemes are not optimal. However, when the number of BS antennas is large, it is shown in [30,31] that linear processing is nearly-optimal. Therefore, in this thesis, we will consider linear processing. The details of linear processing techniques are presented in the following sections.

### 3.5 Linear Receivers (in the Uplink)

With linear detection schemes at the BS, the received signal  $y_{ul}$  is separated into  $K$  streams by multiplying it with an  $M \times K$  linear detection matrix,  $A$ :

$$\widetilde{y}_{ul} = A^H y_{ul} = \sqrt{p_u} A^H H_s + A^H n \dots \dots \dots (3.8)$$

Each stream is then decoded independently. See Figure 3.2. The complexity is on the order of  $K|S|$ . From (3.8), the  $k^{th}$  stream (element) of  $\widetilde{y}_{ul}$ , which is used to decode  $s_k$ , is given by [10]:

$$\widetilde{y}_{ul,k} = \sqrt{p_u} a_k^H h_k s_k + \sqrt{p_u} \sum_{k \neq k}^K a_k^H h_k s_k + a_k^H n \dots \dots \dots (3.9)$$

Where  $a_k$  denotes the  $k^{th}$  column of  $A$ . The interference plus noise is treated as effective noise, and hence, the received signal-to-interference-plus-noise ratio (SINR) of the  $k^{th}$  stream is given by [10]:

$$SINR_k = \frac{p_u |a_k^H h_k|^2}{p_u \sum_{k \neq k}^K |a_k^H h_k|^2 + \|a_k\|^2} \dots \dots \dots (3.10)$$

We now review some conventional linear multiuser receivers.

#### 3.5.1 Maximum-Ratio Combining (MRC) Receiver:

With MRC, the BS aims to maximize the received signal-to-noise ratio (SNR) of each stream, ignoring the effect of multiuser interference. From (3.9), the  $k^{th}$  column of the MRC receiver matrix  $A$  is [10]:

$$\begin{aligned} a_{mrc,k} &= \underset{a_k \in \mathbb{C}^{M \times 1}}{\operatorname{argmax}} \frac{\text{power (desired signal)}}{\text{power (noise)}} \\ &= \underset{a_k \in \mathbb{C}^{M \times 1}}{\operatorname{argmax}} \frac{p_u |a_k^H h_k|^2}{\|a_k\|^2} \dots \dots \dots (3.11) \end{aligned}$$

Since,

$$\frac{p_u |a_k^H h_k|^2}{\|a_k\|^2} \leq \frac{p_u \|a_k\|^2 \|h_k\|^2}{\|a_k\|^2} = p_u \|h_k\|^2$$

And equality holds when  $a_k = \text{constant} \cdot h_k$ , the MRC receiver is:  $a_{mrc,k} = \text{constant} \cdot h_k$ . Plugging  $a_{mrc,k}$  into (3.10), the received SINR of the  $k^{th}$  stream for MRC is given by [10]:

$$SINR_{mrc,k} = \frac{p_u \|h_k\|^4}{p_u \sum_{k \neq k}^K |h_k^H h_k|^2} \dots \dots \dots (3.12)$$

$$\rightarrow \frac{\|h_k\|^4}{\sum_{k \neq k} |h_k^H h_k|^2}, \text{ as } p_u \rightarrow \infty \dots \dots \dots (3.13)$$

### 3.5.2 Zero-Forcing (ZF) Receiver:

By contrast to MRC, zero-forcing (ZF) receivers take the interuser interference into account, but neglect the effect of noise. With ZF, the multiuser interference is completely nulled out by projecting each stream onto the orthogonal complement of the interuser interference. More precisely, the  $k^{th}$  column of the ZF receiver matrix satisfies [10]:

$$\begin{cases} a_{zf,k}^H h_k \neq 0 \\ a_{zf,k}^H h_{\hat{k}} = 0, \forall k \neq \hat{k}. \end{cases} \dots \dots \dots (3.14)$$

The ZF receiver matrix, which satisfies (3.14) for all  $k$ , is the pseudo-inverse of the channel matrix  $H$ . With ZF, we have

$$\tilde{y}_{ul} = (H^H H)^{-1} H^H y_{ul} = \sqrt{p_u} s + (H^H H)^{-1} H^H n \dots \dots \dots (3.15)$$

This scheme requires that  $M \geq K$  (so that the matrix  $H^H H$  is invertible). We can see that each stream (element) of  $\tilde{y}_{ul}$  in (3.15) is free of multiuser interference. The  $k^{th}$  stream of  $\tilde{y}_{ul}$  is used to detect  $s_k$ :

$$\tilde{y}_{ul,k} = \sqrt{p_u} s_k + \tilde{n}_k, \dots \dots \dots (3.16)$$

Where  $\tilde{n}_k$  denotes the  $k$ th element of  $(H^H H)^{-1} H^H n$ . Thus, the received SINR of the  $k^{th}$  stream is given by [10]:

$$SIRN_{zf,k} = \frac{p_u}{[(H^H H)^{-1}]_{kk}} \dots \dots \dots (3.17)$$

### 3.5.3 Minimum Mean-Square Error (MMSE) Receiver:

The linear minimum mean-square error (MMSE) receiver aims to minimize the mean-square error between the estimate  $A^H y_{ul}$  and the transmitted signal  $s$ . More precisely [10],

$$A_{mmse} = \underset{A \in C^{M \times K}}{\operatorname{argmin}} E \{ \|A^H y_{ul} - s\|^2 \} \dots \dots \dots (3.18)$$

$$= \underset{A \in C^{M \times K}}{\operatorname{argmin}} \sum_{k=1}^K E \{ |a_k^H y_{ul} - s_k|^2 \} \dots \dots \dots (3.19)$$

Where  $a_k$  is the  $k^{th}$  column of  $A$ . Therefore, the  $k^{th}$  column of the MMSE receiver matrix is [10]

$$a_{mmse,k} = \underset{a_k \in C^{M \times 1}}{\operatorname{argmin}} E \{ |a_k^H y_{ul} - s_k|^2 \} \dots \dots \dots (3.20)$$

$$= \text{cov}(y_{ul}, y_{ul})^{-1} \text{cov}(s_k, y_{ul})^H \dots\dots\dots (3.21)$$

$$= \sqrt{p_u} (p_u H H^H + I_M)^{-1} h_k \dots\dots\dots (3.22)$$

Where  $\text{cov}(v_1, v_2) \triangleq E\{v_1 v_2^H\}$ ,  $v_1$  and  $v_2$  are two random column vectors with zero-mean elements.

It is known that the MMSE receiver maximizes the received SINR. Therefore, among the MMSE, ZF, and MRC receivers, MMSE is the best. We can see from (3.22) that, at high SNR (high  $p_u$ ), ZF approaches MMSE, while at low SNR, MRC performs as well as MMSE. Furthermore, substituting (3.22) into (3.10), the received SINR for the MMSE receiver is given by [10]:

$$\text{SINR}_{\text{mmse},k} = p_u h_k^H \left( p_u \sum_{i \neq k}^K h_i h_i^H + I_M \right)^{-1} h_k \dots\dots\dots (3.23)$$

### 3.6 Linear Precoders (in the Downlink)

In the downlink, with linear precoding techniques, the signal transmitted from  $M$  antennas  $x$ , is a linear combination of the symbols intended for the  $K$  users. Let  $q_k$ ,  $E\{|q_k|^2\} = 1$ , be the symbol intended for the  $k^{\text{th}}$  user. Then, the linearly precoded signal vector  $x$  is [10]:

$$x = \sqrt{\alpha} W q, \dots\dots\dots (3.24)$$

Where  $q = \triangleq [q_1 q_2 \dots \dots q_K]^T$ ,  $W \in C^{M \times K}$  is the precoding matrix and  $\alpha$  is a normalization constant chosen to satisfy the power constant  $E\{\|x\|^2\} = 1$ . Thus,

$$\alpha = \frac{1}{E\{\text{tr}(W W^H)\}}, \dots\dots\dots (3.25)$$

A block diagram of the linear precoder at the BS is shown in Figure 3.3.

Plugging (3.24) into (3.4), we obtain

$$y_{dl,k} = \sqrt{\alpha p_d} h_k^T W q + z_k \dots\dots\dots (3.26)$$

$$= \sqrt{\alpha p_d} h_k^T w_k q_k + \sqrt{\alpha p_d} \sum_{k \neq k}^K h_k^T w_k q_k + z_k \dots\dots\dots (3.27)$$

Therefore, the SINR of the transmission from the BS to the  $k^{\text{th}}$  user is

$$SINR_k = \frac{\alpha p_d |h_k^T w_k|^2}{\alpha p_d \sum_{k \neq k}^K |h_k^T w_k|^2 + 1}. \quad \dots\dots\dots (3.28)$$

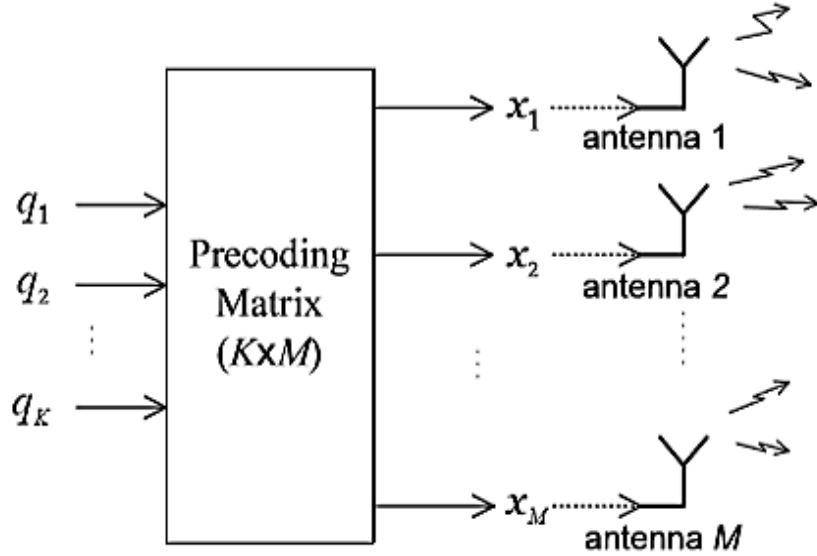


Figure 3.3: Block diagram of the linear precoders at the BS [12].

Three conventional linear precoders are maximum-ratio transmission (MRT), ZF, and MMSE precoders. These precoders have similar operational meanings and properties as MRC, ZF, MMSE receivers, respectively. Thus, here we just provide the final formulas for these precoders, i.e.,

$$W = \begin{cases} H^*, & \text{for MRT} \\ H^*(H^T H^*)^{-1}, & \text{for ZF} \\ H^* \left( H^T H^* + \frac{K}{p_d} I_K \right)^{-1}, & \text{for MMSE} \end{cases} \quad \dots\dots\dots (3.29)$$

### 3.7 Circuit Power Consumption Model

The Circuit power consumption  $P_{CP}$  is the sum of the power consumed by different analog components and digital signal processing [32]. The network model to show that a PC model accounting for the transmit power as well as for the CP consumed by the transceiver hardware at the BS and UEs is necessary to avoid misleading conclusions about the EE. These are not the only contributions that must be taken into account to appropriately evaluate the CP of the UL and DL of Massive MIMO. We will show that we must also consider the power consumed by digital signal processing,

backhaul signaling, encoding, and decoding [33]. Building on [10, 32 - 36] a CP model for a generic BS in a Massive MIMO network is:

$$P_{CP} = P_{FIX} + P_{TC} + P_{CE} + P_{C/D} + P_{BH} + P_{LP} \quad \dots \dots \dots (3.30)$$

Where  $P_{FIX}$  defined before as a constant quantity accounting for the fixed power was required for control signaling and load-independent power of backhaul infrastructure and baseband processors. Furthermore,  $P_{TC}$  accounts for the power consumed by the transceiver chains,  $P_{CE}$  for the channel estimation process performed once per coherence block,  $P_{C/D}$  for the channel encoding and decoding units,  $P_{BH}$  for the load dependent backhaul signaling, and  $P_{LP}$  for the linear signal processing at the BS. Note that neglecting the power consumed by transceiver chains, channel estimation, precoding, and combining was previously the norm in multiuser MIMO. More precisely, the small numbers of antennas and UEs, before Massive MIMO was introduced, were such that the CP for all those operations was negligible compared to the fixed power. The CP associated with those operations was modeled for single-cell systems in [10, 36], while multicellular systems were considered in [37]. Inspired by these works, we provide in what follows a tractable and realistic model for each term in (3.30), as a function of the main system parameters  $M$  and  $K$ . This is achieved by characterizing the hardware setup using a variety of fixed hardware coefficients, which are kept generic in the analysis; typical values will be given later and strongly depend on the actual hardware equipment and the state-of-the-art in circuit implementation.

### 3.7.1 Transceiver Chains

As described in [10] and [40], the power consumption  $P_{TC}$  of a set of typical transmitters and receivers can be quantified as

$$P_{TC} = MP_{BS} + P_{SYN} + KP_{UE} \quad \dots \dots \dots (3.31)$$

Where  $P_{BS}$  is the power required to run the circuit components such as converters, mixers, and filters attached to each antenna at the BS and  $P_{SYN}$  is the power consumed by the local oscillator. The last term  $P_{UE}$  accounts for the power required by all circuit components such as amplifiers, mixer, oscillator, and filters of each single-antenna UE.  $M$  and  $K$  denote by the number of antenna array at BS and number of user.

### 3.7.2 Channel Estimation

All processing is carried out locally at the BS and UEs, whose computational efficiency are  $L_{BS}$  and  $L_{UE}$  arithmetic complex-valued operations per Joule respectively. There are  $\frac{B}{U}$  coherence blocks per second and the pilot-based CSI estimation is performed once per block. In the uplink, the BS receives the pilot signal as an  $M \times \tau^{(ul)}$   $K$  matrix and estimates

each UE's channel by multiplying with the corresponding pilot sequence of length  $\tau^{(ul)}K$  [40]. This standard linear algebra operation [39] and requires  $P_{CE}^{(ul)} = \frac{B}{U} \frac{2\pi^{(ul)}MK^2}{L_{BS}}$  Watt. In the downlink, each active UE receives a pilot sequence of length  $\tau^{(dl)}K$  and processes it to acquire its effective precoded channel gain one inner product and the variance of interference plus noise one inner product. From [39], we obtain  $P_{CE}^{(dl)} = \frac{B}{U} \frac{4\pi^{(dl)}K^2}{L_{UE}}$  Watt. Therefore, the total power consumption of the channel estimation process becomes [10]:

$$P_{CE} = P_{CE}^{(ul)} + P_{CE}^{(dl)}$$

$$P_{CE} = P_{CE}^{(ul)} = \frac{B}{U} \frac{2\pi^{(ul)}MK^2}{L_{BS}} + P_{CE}^{(dl)} = \frac{B}{U} \frac{4\pi^{(dl)}K^2}{L_{UE}} \quad \dots \dots \dots (3.32)$$

Where  $P_{CE}^{(ul)}$  is the uplink channelestimationprocess,  $P_{CE}^{(dl)}$  is the downlink channelestimationprocess.

### 3.7.3 Coding and Decoding

In the downlink, the BS applies channel coding and modulation to  $K$  sequences of information symbols and each UE applies some suboptimal fixed-complexity algorithm for decoding its own sequence. The opposite is done in the uplink. The power consumption  $P_{C/D}$  accounting for these processes is proportional to the number of bits [10, 40] and can thus be quantified as:

$$P_{C/D} = \sum_{k=1}^K \left( E \{ R_k^{(ul)} + R_k^{(dl)} \} \right) (P_{COD} + P_{DEC}) \quad \dots \dots \dots (3.33)$$

where  $P_{COD}$  and  $P_{DEC}$  are the coding and decoding powers in Watt per bit/s,  $R_k^{(ul)}$  and  $R_k^{(dl)}$  are uplink and downlink user gross rates respectively. For simplicity, we assume that  $P_{COD}$  and  $P_{DEC}$  are the same in the uplink and downlink, but it is straightforward to assign them different values.

### 3.7.4 Backhaul

The backhaul is used to transfer uplink/downlink data between the BS and the core network. The power consumption of the backhaul is commonly modeled as the sum of two parts [10]: one load-independent and one load-dependent. The first part was already included in  $P_{FIX}$ , while the load-dependent part is proportional to the average sum rate. Looking jointly at the downlink and uplink, the load-dependent term  $P_{BH}$  can be computed as [38]:

$$P_{BH} = \sum_{k=1}^K \left( E \{ R_k^{(ul)} + R_k^{(dl)} \} \right) P_{BT} \quad \dots \dots \dots (3.34)$$

where  $P_{BT}$  is the backhaul traffic power in Watt per bit/s,  $R_k^{(ul)}$  and  $R_k^{(dl)}$  are uplink and downlink user gross rate.

### 3.7.5 Linear Processing

The transmitted and received vectors of information symbols at the BS are generated by transmit precoding and processed by receive combining, respectively. This costs [39]

$$P_{LP} = B \left( 1 - \frac{(\tau^{(ul)} + \tau^{(dl)})K}{U} \right) \frac{2MK}{L_{BS}} + P_{LP-C} \quad \dots \dots \dots (3.35)$$

where the first term describes the power consumed by making one matrix-vector multiplication per data symbol and  $L_{BS}$  is computational efficiency at BSs. The second, term,  $P_{LP-C}$ , accounts for the power required for the computation of  $G$  and  $V$ . The precoding and combining matrices are computed once per coherence block and the complexity depends strongly on the choice of processing scheme. Since  $G = V$  is a natural choice except when the uplink and downlink are designed very differently, we only need to compute one of them and thereby reduce the computational complexity. If MRT/MRC is used, we only need to normalize each column of  $H$ . This requires approximately [10]:

$$P_{LP-C}^{(MRT/MRC)} = \frac{B}{U} \frac{3MK}{L_{BS}} \quad \dots \dots \dots (3.36)$$

which was calculated using the arithmetic operations for standard linear algebra operations in [39]. On the other hand, if ZF processing is selected, then approximately [10]:

$$P_{LP-C}^{(ZF)} = \frac{B}{U} \left( \frac{K^3}{3L_{BS}} + \frac{3MK^2 + MK}{L_{BS}} \right) \quad \dots \dots \dots (3.37)$$

is consumed, if the channel matrix inversion implementation is based on standard Cholesky factorization and back-substitution [39]. The computation of optimal MMSE processing is more complicated since the power allocation in is a fixed-point equation that needs to be iterated until convergence. Such fixed-point iterations usually converge very quickly, but for simplicity we fix the number of iterations to some predefined number  $Q$ . This requires  $P_{LP-C}^{(MMSE)} = Q P_{LP-C}^{(ZF)}$  Watt since the operations in each iteration are approximately the same as in ZF.

### 3.8 Comparison of CP with Different Processing Schemes

We will compare the CP consumed with different combining/precoding schemes. There are  $M$  antennas at each BS and  $K$  user in each cell. The number of samples per coherence block that is used for data is  $\tau_c$  and  $\tau_p$ , whereof 1/3 is used for UL and 2/3 for DL. We consider UL and DL transmit powers of 20 dBm per UE. The Gaussian local scattering with ASD  $\sigma_\phi$  is used as channel model. The throughput of cell for computing the consumed power for backhaul, encoding, and decoding are obtained using the UL and DL. Computational complexity per coherence block of different receives combining schemes [28]:

Table I: Computational Complexity for Different Receives Combining Schemes.

Linear Precoding Methods	Computing combining vectors Multiples
MMSE	$\sum_{l=1}^L \frac{(3M_j^2 + M_j) K_l}{2} + \frac{M_j^3 - M_j}{3} + M_j \tau_p (\tau_p - K_j)$
ZF	$\frac{3K_j^2 M_j}{2} + \frac{K_j M_j}{2} + \frac{K_j^3 - K_j}{3}$
MRC / MRT	$\frac{K_j M_j}{2} + \frac{K_j^3 - K_j}{3}$

Power required by each BS for the signal processing with different combining / precoding schemes over a bandwidth  $B$ , under the assumption that the precoding vectors are chosen as normalized versions of the receive combining vectors [28]:

Table II: Power Required for Each BS with Different Combining Precoding Scheme.

Linear Precoding Methods	$P_{UL}$	$P_{DL}$
MMSE	$\frac{3B}{\tau_c L_{BS}} \left( \sum_{l=1}^L \frac{(3M_j^2 + M_j) K_l}{2} + \frac{M_j^3}{3} + 2M_j + M_j \tau_p (\tau_p + K_j) \right)$	$\frac{3B}{\tau_c L_{BS}} M_j K_j$

ZF	$\frac{3B}{\tau_c L_{BS}} \left( \sum_{l=1}^L \frac{3K_j^2 M_j}{2} + \frac{K_j M_j}{2} + \frac{K_j^3 - K_j}{3} + 2M_j + \frac{7}{3} K_j \right)$	$\frac{3B}{\tau_c L_{BS}} M_j K_j$
MRC / MRT	$\frac{7B}{\tau_c L_{BS}} K_j$	$\frac{3B}{\tau_c L_{BS}} M_j K_j$

### 3.9 Tradeo□ between Power Consumption (PC) and Throughput

The tradeo□ between PC and throughput, using the CP model introduced in the previous section and the sets of CP values reported in Table 3. We focus on the PC and throughput of the Massive MIMO system to stress that one can't complete EE examination without determining the data transfer capacity. There are M antennas at each BS and K UEs in each cell. The values of M and K will be changed and specified in each figure. The quantity of samples consistent with coherence block used for UL and DL are  $\tau_u = \frac{1}{3}(\tau_c - \tau_p)$  and  $\tau_d = \frac{2}{3}(\tau_c - \tau_p)$ , respectively. We take into account UL and DL transmit powers of 20 dBm in step with UE. The throughput is acquired as in with the aid of using the UL and DLSE expressions.

The EE of cell is computed as:

$$EE = \frac{TR}{ETR + CP} \dots\dots\dots (3.38)$$

Where ETP denotes the E□ective Transmit Power of cell, TR denotes throughput of cell and CP denotes consumed power of cell BSs. This term accounts for the power consumed by the transmission of the pilot sequences as well as of UL and DL signals:

$$ETR = \frac{\tau_p}{\tau_c} \sum_{k=1}^K \frac{1}{\mu_{UE,k}} p_k + \frac{\tau_u}{\tau_c} \sum_{k=1}^K \frac{1}{\mu_{UE,k}} p_k + \frac{1}{\mu_{BS}} \frac{\tau_d}{\tau_c} \sum_{k=1}^K p_k \dots\dots\dots (3.39)$$

Where  $\mu_{UE, k}$  is the PA e□iciency at UE k in cell and  $\mu_{BS, j}$  is that of BS.

The throughput of cell for computing the consumed power for backhaul, encoding, and interpreting is gotten utilizing the UL and DL SE articulations. For each plan and number of antennas, we utilize the limit destined for the UL and the one that gives the biggest SE between those of the DL:

$$TR = B \sum_{k=1}^K (SE_k^{UL} + \max(SE_k^{DL}, SE_k^{DL})) \dots\dots\dots (3.40)$$

Where B is the Transmission Bandwidth,  $SE_k^{UL}$  and  $SE_k^{DL}$  are the Spectral Efficiency of uplink and downlink system per user.

### 3.10 Problem Statement

The EE of a communication system is measured in bit/Joule [16] and is computed as the ratio between the average sum rate (in bit/second) and the average total power consumption  $P_T$  (in Watt = Joule/second). In a multi-user setting, the total EE metric accounting for both uplink and downlink takes the following form.

The total EE of the uplink and downlink is

$$EE = \frac{\sum_{k=1}^K \left( E\{R_k^{(ul)}\} + E\{R_k^{(dl)}\} \right)}{P_{TX}^{(ul)} + P_{TX}^{(dl)} + P_{CP}} \dots \dots \dots (3.41)$$

Where  $P_{CP}$  accounts for the circuit power consumption,  $R_k^{(ul)}$  and  $R_k^{(dl)}$  are uplink and downlink user gross rate,  $P_{TX}^{(ul)}$  and  $P_{TX}^{(dl)}$  are total power required for uplink and downlink system.

In most of the existing works,  $P_{CP}$  is modeled as  $P_{CP} = P_{FIX}$  where the term  $P_{FIX}$  is a constant quantity accounting for the fixed power consumption required for site-cooling, control signaling, and load-independent power of backhaul infrastructure and baseband processors [16]. Hence, the simplified model  $P_{CP} = P_{FIX}$  gives the impression that we can achieve an unbounded EE by adding more and more antennas. This modeling artifact comes from ignoring that each antenna at the BS requires dedicated circuits with non-zero power consumption, and that the signal processing tasks also become increasingly complex.

In other words, an accurate modeling of  $P_{CP}$  is of paramount importance when dealing with the design of energy-efficient communication systems. The next section aims at providing an appropriate model for  $P_{CP}(M, K, \bar{R})$  as a function of the three main design parameters: the number of BS antennas (M), number of active UEs (K), and the user gross rates ( $\bar{R}$ ).

### 3.10.1 Problem Solutions:

An EE-optimal multi-user MIMO setup is achieved by solving the following optimization problem:

$$\underset{M \in Z_+, K \in Z_+, \bar{R} \geq 0}{\text{maximize}} EE = \frac{\sum_{k=1}^K \left( E\{R_k^{(ul)}\} + E\{R_k^{(dl)}\} \right)}{P_{TX}^{(ul)} + P_{TX}^{(dl)} + P_{CP}(M, K, \bar{R})} \dots \dots \dots (3.42)$$

This Problem is solved analytically for Linear Precoding Methods.

1. Observe that prior works on EE optimization have focused on either uplink or downlink.

2. Problem is an optimization in which the total EE is maximized for given fractions UL and DL of uplink and downlink Transmissions.
3. Maximizing the EE in does not mean decreasing the total power, but to pick a good power level and use it wisely.

## Chapter 04

### Simulation and Result Analysis

#### 4.1 Why Simulation?

Simulation is defined as the process of creating a model of an existing or proposed system in order to identify and understand their functioning. We can predict the estimation and assumption of the real system by using simulation results.

#### 4.2 Simulator

In this thesis, the theoretical analysis presented previously, we conducted a system level simulation using a MATLAB 2015a.

#### 4.3 Implementation of the Model

The implementation consists of three main programs:

**The Linear Precoding Method:** In the linear precoding function, the inputs are: number of antenna ( $M$ ), number of users ( $K$ ), the channel matrix  $H$  and the output signal  $W$ . By implementing equation (3.29), we estimate the number of complex multiplication from channel matrix function. For linear precoding calculation, MATLAB simulator first calculates the response channel matrix and inverse channel matrix function according to formula and table 3.1 with respect to number of antenna and users. Finally, this function evaluates the number of complex multiplication response for different linear precoding methods.

**The Total Circuit Power (CP) Consumption:** In the Total Circuit Power Consumption function, the given inputs: the fixed power of BS ( $P_{\text{FIX}}$ ), the power consumed by the transceiver chains ( $P_{\text{TC}}$ ), the channel estimation process performed once per coherence block ( $P_{\text{CH}}$ ), the load dependent backhaul signaling ( $P_{\text{BH}}$ ), the linear signal processing at the BS ( $P_{\text{LP}}$ ) and the output signal ( $P_{\text{CP}}$ ). By implementing equation (3.30), we calculate the total circuit power consumption. For calculate total circuit power consumption with different linear precoding methods, MATLAB simulator first calculates the circuit power consumption according to formula and table 3.2 with respect to number of antenna and users. Finally, this function evaluates the total circuit power consumption response for different linear precoding methods.

**The Maximize Energy Efficiency (EE):** In the maximize Energy Efficiency (EE) function, the given inputs: uplink and downlink gross rate, uplink and downlink transmit power, total circuit power consumption and the output signal EE. By implementing

equation (3.38 and 3.39), we calculate the maximize Energy Efficiency (EE) for different linear precoding methods.

#### 4.4 Purpose of the Simulation:

The goal of the simulation is get maximum energy efficiency (EE) with the proposed method. The simulation scenarios enable analysis of different precoding estimator performance to find the optimal numbers of antenna (M) and numbers of users (K) with maximize energy efficiency. In our simulation, on EE optimizations have focused on uplink and downlink transmissions process. In this thesis is to compare the various linear precoding algorithms for maximum energy efficiency with respect to numbers of antenna (M), numbers of users (K) and total circuit power ( $P_{CP}$ ). Thus, the accurate goal will be achieved.

#### 4.5 Simulation Parameters

The corresponding simulation parameters are given Table 3.

Table III: Simulation Parameters

Parameter	Value
Number of Antenna	200
Number of Users	100
Transmission Bandwidth (B)	20 MHz
Coherence Bandwidth ( $B_C$ )	180 kHz
Coherence Time ( $T_C$ )	10 ms
Coherence Block ( $\tau_c$ )	400
Computational Efficiency at BSs ( $L_{BS}$ )	12.8 Gflops/W
UL Transmit Power ( $P_{UL}$ )	20 dBm
DL Transmit Power ( $P_{DL}$ )	20 dBm
Fixed Power Consumption ( $P_{FIX}$ )	9 W
Power for BS LO: $P_{LO}$	0.1 W

Power of Circuit Components (such as converters, mixers, and filters) ( $P_{BS}$ )	1 W
Power consumed by Local Oscillator at BSs ( $P_{SYN}$ )	1 W
Power required of circuits components of each single-antenna UE. ( $P_{UE}$ )	0.1 W
Power for data encoding ( $P_{COD}$ )	0.01 W
Power for data decoding ( $P_{DEC}$ )	0.08 W
Power for backhaul tra□c ( $P_{BT}$ )	0.025 W

#### 4.6 Analysis of Simulation Result: Complex Multiplications per Coherence Block with Different Precoding Schemes.

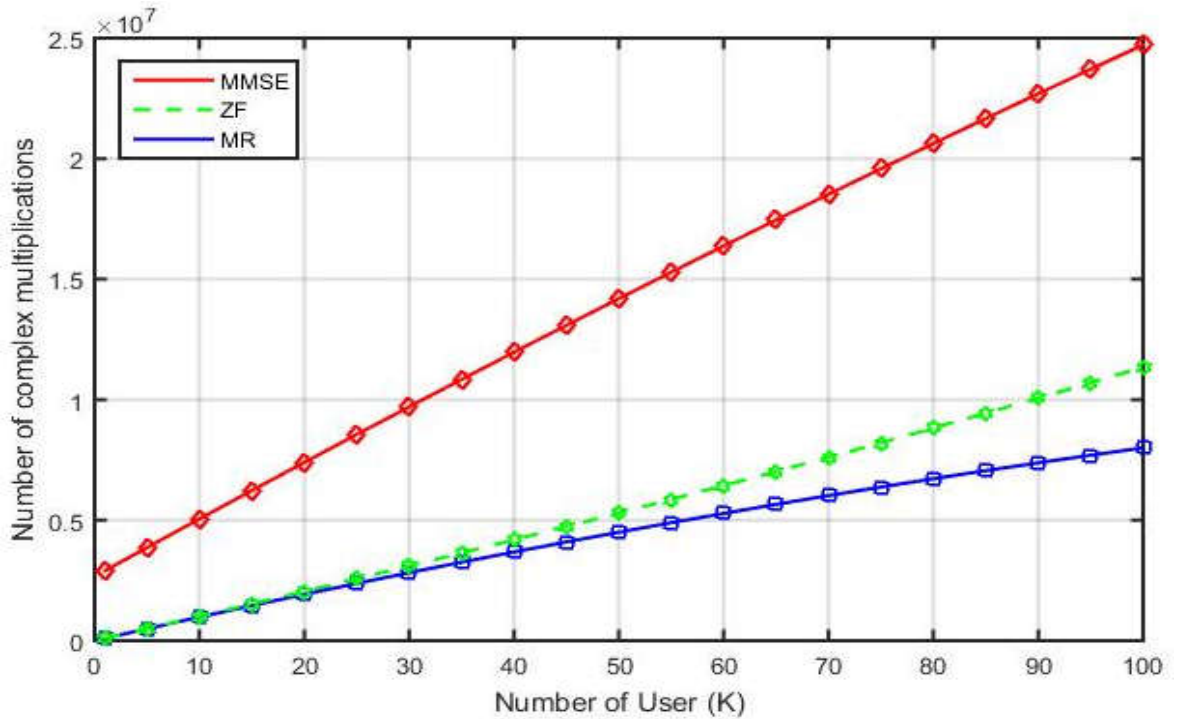


Figure 4.1: Number of complex multiplications per cell when using different combining methods with varies K and Fixed M

In Figure 4.1 and 4.2 illustrate the number of complex multiplications per coherence block as a function of either the number of UEs or the number of BS antennas. In Figure 4.1 we assume that  $K \in [1,100]$  and  $M = 200$  in every cell. On the other hand, in Figure

4.2 we consider  $K = 100$  and let  $M$  vary from 0 to 200. The complexity increases with the number of UEs and BSs antennas for all combining schemes.

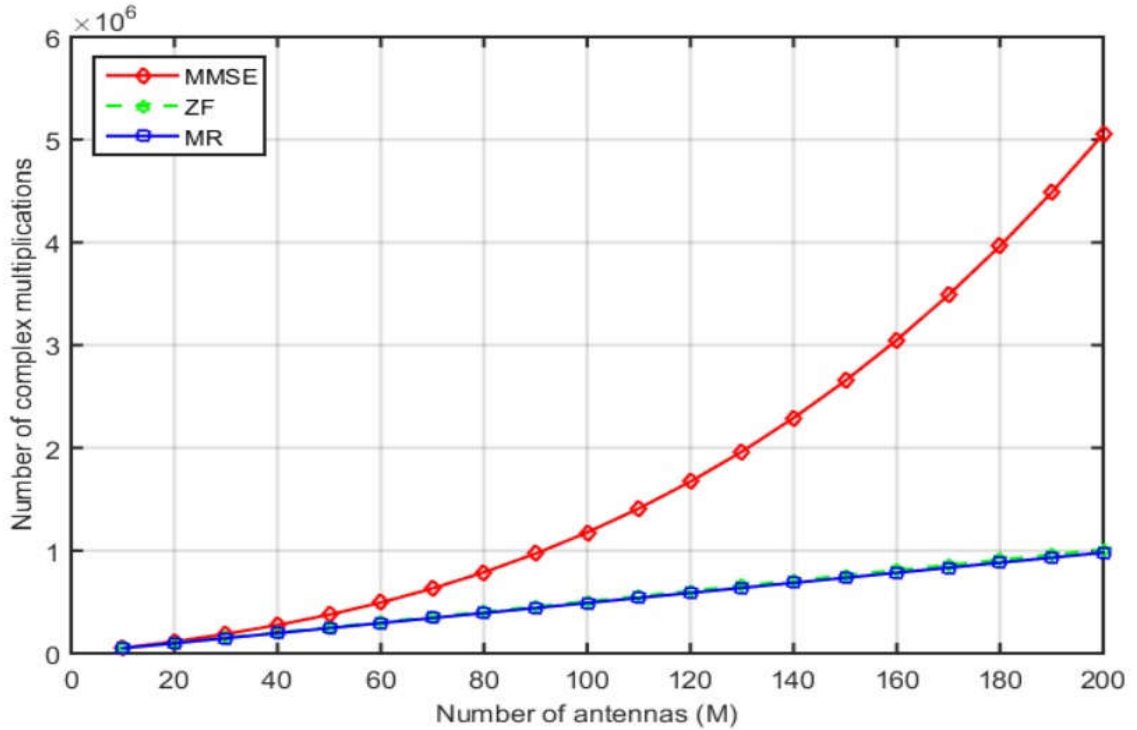


Figure 4.2: Number of complex multiplications per cell when using different combining methods with varies  $M$  and Fixed  $K$

MMSE has clearly the highest complexity. ZF provide even lower complexity than MMSE since these schemes invert substantially smaller  $K_j \times K_j$  matrices (compared to the  $M_j \times M_j$  matrices that are inverted by MMSE). MR provides the lowest computational complexity since no matrix inverses are computed, which also means that all computations can be parallelized in the implementation a separate processing core can be used per antenna and UE.

Table IV: Number of Complex Multiplications per cell when using Different Combining Methods with Varies  $K$  and Fixed  $M$

Linear Precoding Method	Value
MMSE	$2.472e+07 = 13.72$
ZF	$1.134e+07 = 10.08$
MRC	$1.125e+06 = 9.06$

Table V: Number of Complex Multiplications per cell when using Different Combining Methods with Varies M and Fixed K

Linear Precoding Method	Value
MMSE	$5.052e+06 = 19.73$
ZF	$1.011e+06 = 8.75$
MRC	$0.98e+05 = 7.66$

Table VI: Comparison of Complex Multiplications per cell with Reference Paper [28]:

Linear Precoding Methods		Data from Table IV (W)	Data from Table V (W)
This Work	MMSE	$2.472e+07 = 13.72$	$5.052e+06 = 19.73$
	ZF	$1.134e+07 = 10.08$	$1.011e+06 = 8.75$
	MRT/MRC	$1.125e+06 = 9.06$	$0.98e+05 = 7.66$
Reference Paper [28]	MMSE	$3.393e+06 = 15.22$	$6.128e+06 = 22.65$
	ZF	$2.033e+05 = 10.53$	$2.058e+05 = 10.59$
	MRT/MRC	$1.84e+05 = 10.00$	$1.9e+05 = 10.16$

#### 4.7 Analysis of Simulation Result: The Total CP per cell for the Combined UL and DL Scenario with Different precoding schemes.

In Figures 4.3 & 4.4 illustrates the total CP per cell for the combined UL and DL scenario with different combining/precoding schemes. In Figure 4.3: we consider  $M = 200$  and let  $K$  vary from 0 to 100. The CP increases with the number of UEs. MMSE requires the highest CP and MR the lowest. In Figure 4.4: we consider  $K = 100$  and let  $M$  vary from 0 to 200. The CP increases with  $M$  for all schemes. The highest CP is required by MMSE. This is mainly due to the increased computational efficiency. ZF consume less CP, since invert matrices of dimensions  $K \times K$ , rather than  $M \times M$ . MR is characterized by the lowest CP since no matrix inversions are required. MR only provides a substantial complexity reduction when the number of UEs is very large.

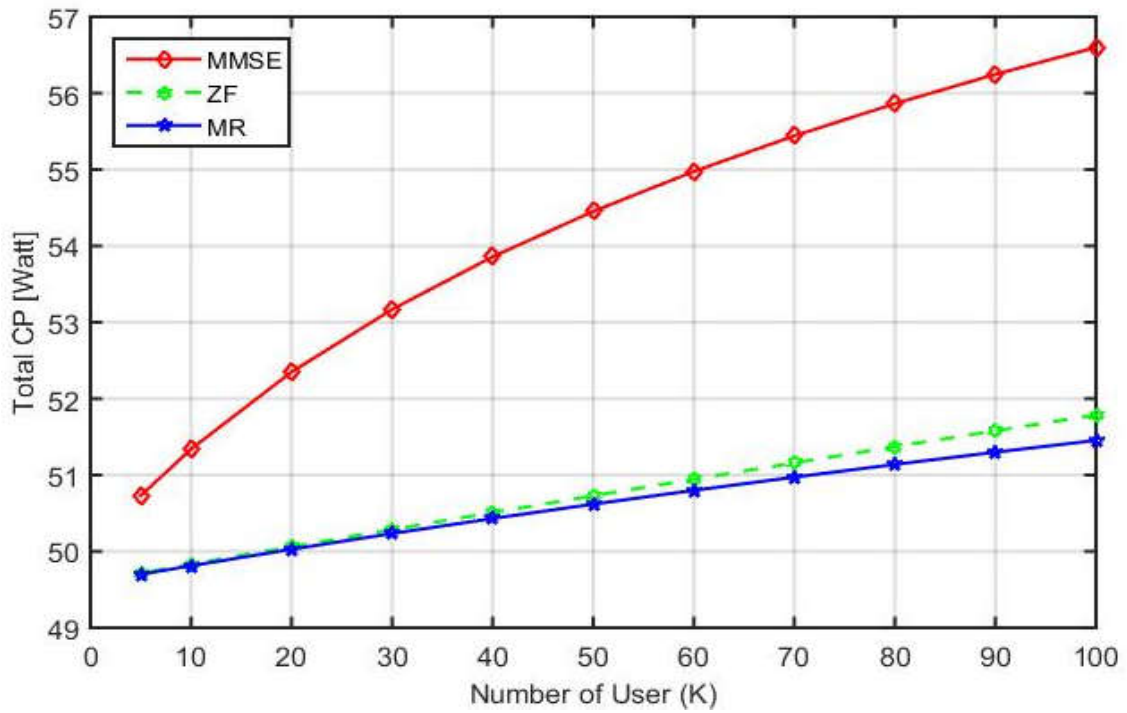


Figure 4.3: Total CP vs. Number of Users (K) when using different combining methods with fixed antenna (M).

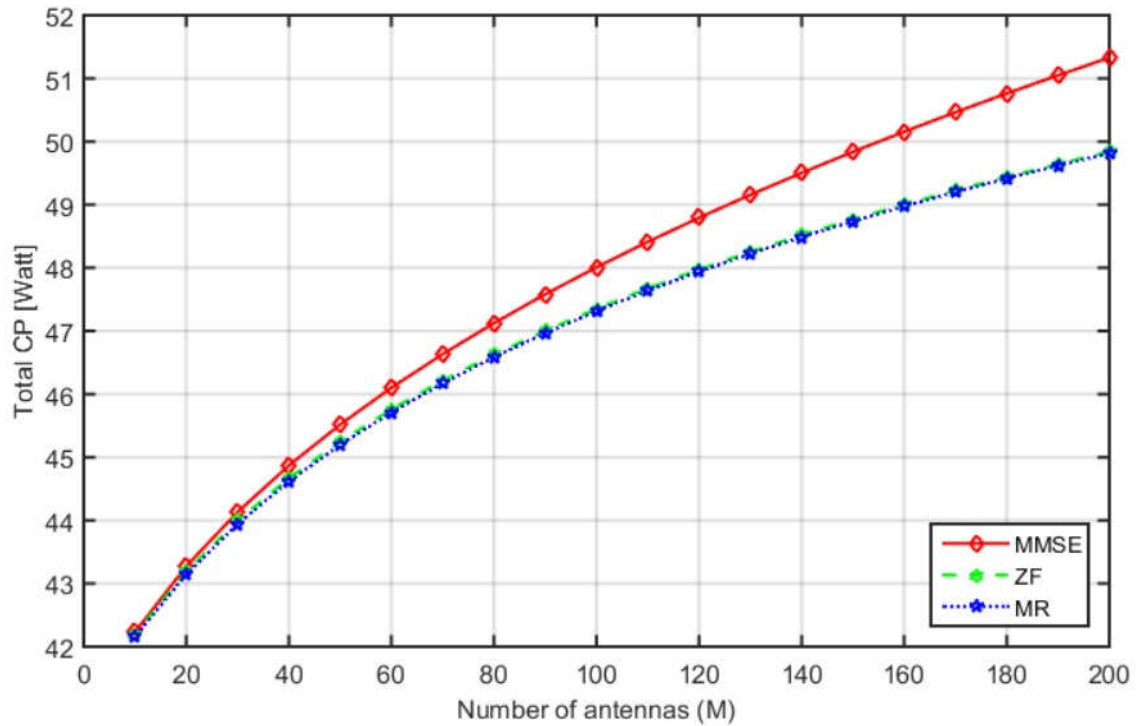


Figure 4.4: Total CP vs. Number of antenna (M) when using different combining methods with Fixed Users (K).

The CP of all schemes, for the two different sets of parameter values,  $M = 200$ , and  $K = 100$  are summarized in Table VII & VIII. As we can see, in this considered setup the CP required by the different schemes is marginally different. This happens because the CP of the transceiver hardware dominates over that of signal processing. The CP contributed by the fixed power, Transceiver chains, Signal processing for UL reception, DL transmission and Precoding computation are the same for all schemes.

Table VII: Total CP per cell of both UL and DL for fixed user ( $K$ ) and varying number of antennas ( $M$ ).

Methods	Value [Watt]
MMSE	51.33
ZF	49.84
MR	49.83

Table VIII: Total CP per cell of both UL and DL for fixed number of antennas ( $M$ ) and varying user ( $K$ ).

Methods	Value [Watt]
MMSE	49.53
ZF	47.72
MR	47.64

Table IX: Comparison of Total CP with Reference Paper [28]:

Linear Precoding Methods		Average CP vale of UL and DL Data from Table VII & VIII
This Work	MMSE	50.43
	ZF	48.78
	MRT/MRC	48.74
Reference Paper [28]	MMSE	56.35
	ZF	54.43
	MRT/MRC	53.96

## 4.8 Analyzed the Average SE per cell for the Combined UL and DL Scenario with Different Precoding Schemes.

In MRC, the multiple antenna transmitters use the channel estimate of a terminal to maximize the strength of that terminal's signal by adding the signal components coherently. MRC precoding maximizes the SNR and works well in the massive MIMO system, since the base station radiates low signal power to the users on average. ZF precoding is a method of spatial signal processing by which the transmitter can null out multiuser interference signals. In general, ZF precoder performs well under high SNR conditions. The ZF precoder outperforms MRC, as shown in Figure 4.5 in performance as well as in computational complexity. It also suppresses inter-cell interference at the cost of reducing the array gain [6]. It is noted that spectral efficiency increases as the number of BS antennas grows. In addition, the figure shows the superiority of the performance of MMSE, especially in massive MIMO. MMSE precoding is the optimal linear precoding in a massive MIMO downlink and uplink system. This technique uses the mean square error (MSE). The Lagrangian technique is used to optimize this precoder, using the average power of each transmitting antenna as the constraint.

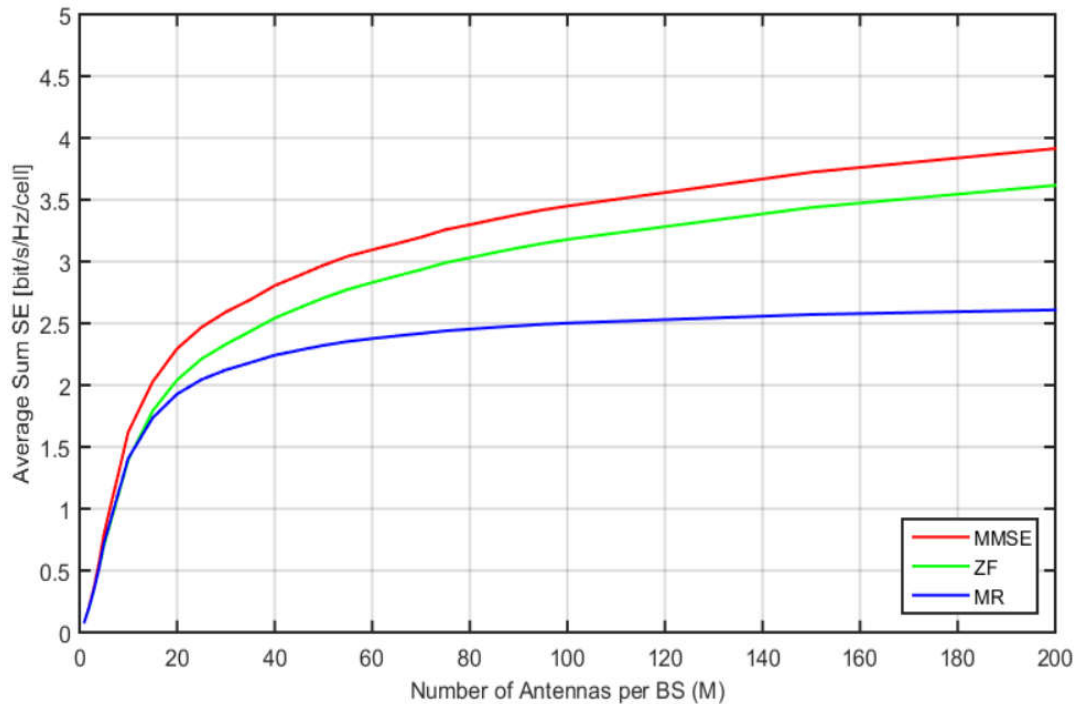


Figure 4.5: Average DL and UL sum SE as a function of the number of BS antennas for different precoding schemes.

Now we compare the average SE achieved with different precoding schemes. We consider  $K = 10$  users per cell and a varying number of BS antennas. Equal DL and UL power

allocation of 20 dBm per UE. For each scheme and number of antennas, we use the DL and UL capacity bound and pilot reuse factor  $f \in 1$ , that gives the largest SE. Figure 4.5 shows the average DL and UL sum SE with  $f = 1$ . We consider MMSE, ZF and MRC precoding. MMSE provides the highest SE (SE = 3.917) for any number of antennas. ZF provides almost the same SE (SE = 3.605). Finally, MRC provides the lowest SE (SE = 2.617) among all schemes and it is also the only scheme that prefers the hardening bound over the estimation bound.

As in the average SE of DL and UL, the computational complexity is higher for the precoding/combining schemes that provide higher SEs, and we can appoint MMSE, ZF and MRC as three distinct tradeoffs between high SE and low complexity. These are the schemes to choose between in a practical implementation.

#### 4.9 Analyzed the Power Consumption (PC) and Throughput with different precoding schemes.

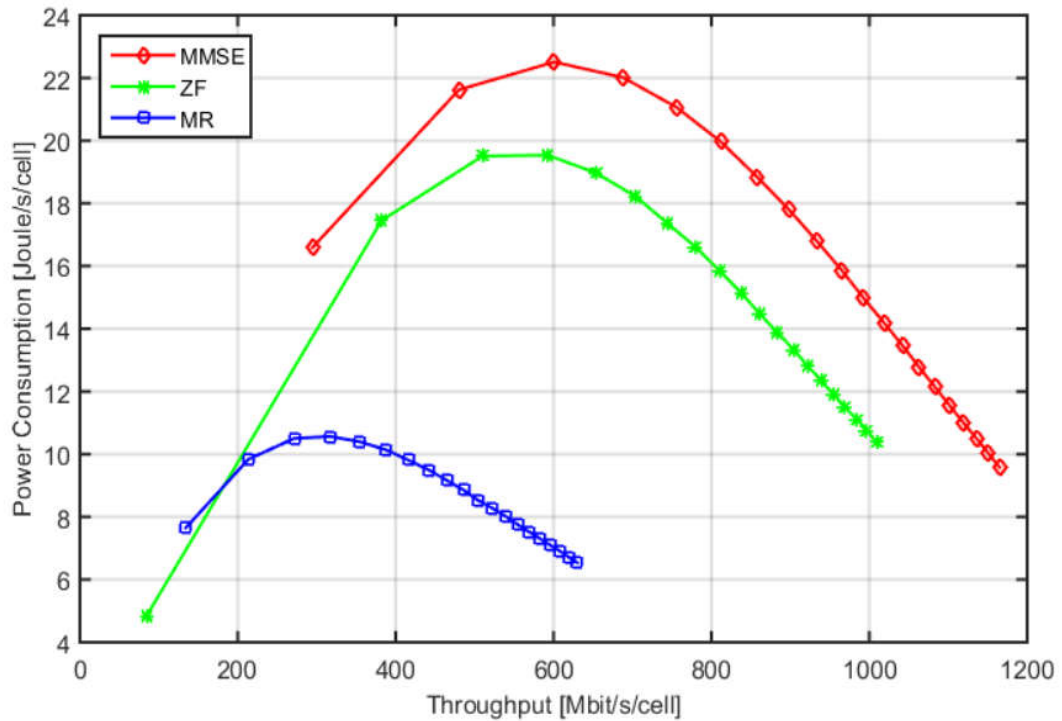


Figure 4.6: PC versus throughput for function of the different precoding schemes.

Figure 4.6 illustrates the PC as a function of the average throughput per cell with all processing schemes. The different throughput values are achieved with  $K = 10$  UEs and by letting the number of BS antennas vary from  $M = 10$  to  $M = 200$ . We notice that the PC is a unimodal function of the throughput for all schemes and both sets of CP values. This implies that we can jointly increase the throughput and PC up to the maximum point, but

further increases in throughput can only come at a loss in PC. The curves are quite smooth around the maximum PC point; thus, there are a variety of throughput values or, equivalently, numbers of BS antennas that provide nearly maximum PC. MMSE provides the highest PC for any value of the throughput. MR has the lowest performance. This shows that, in the considered setup, the additional computational complexity of MMSE processing pays off both in terms of SE.

From Figure 4.6, we can see that the maximal PC value with MMSE is 22.51 Joule/s/cell is achieved at throughput of 600.8 Mbit/s/cell. MR has performance the lowest PC value is 10.57 Joule/s/cell is achieved at throughput of 317 Mbit/s/cell. ZF provides a maximum PC of 19.54 Joule/s/cell is achieved at throughput of 592.7 Mbit/s/cell. Interestingly, ZF and MR tend to perform as MMSE when the throughput increases. This happens since the higher the throughput, the higher is also the CP, due to the larger number of antennas.

#### 4.10 Network Design for Maximal Energy Efficiency

In the previous section, we discussed the complex multiplications, total circuit power (CP), average sum Spectral Efficiency (SE), Power Consumption (PC) and Throughput of Massive MIMO networks for a given number of UEs and varying number of BS antennas. In the following, we look at the EE from a different perspective: we design the network from scratch to achieve maximal EE, without assumptions on the number of antennas or UEs. We focus the following questions:

- a. What is the optimal number of BS antennas?
- b. How many UEs should be served?
- c. When different processing schemes should be used?

Figure 4.7, 4.8 and 4.9 show that the set of achievable maximum energy efficiency (EE) values with different linear precoding methods. In figure 4.7, MMSE precoding method get the maximum energy efficiency values other precoding methods. With MMSE, a maximal EE of 24.16 Mbit/Joule is achieved by  $(M, K) = (50, 30)$ . In figure 4.8, ZF precoding method gets the slightly less maximum energy efficiency value than MMSE. The corresponding set of achievable a maximal EE of 22.96 Mbit/Joule is achieved by  $(M, K) = (80, 30)$ . Interestingly, MRT precoding method shows a very different behavior: the energy efficiency value is much smaller than with MMSE and ZF which is 11.77 Mbit/Joule achieved at  $(M, K) = (50, 20)$ . The MMSE gives better performance because the MMSE is able to make the massive MIMO system less sensitive to SNR at an increased number of antennas for achievable data rates compared with ZF and MRT, where an MMSE and ZF are able to work at high SNR. Consequently, EE first increases and then decreases with an increased number of antennas, which maximizes the transmit power when taking into account the consumption circuit power and the transmit power.

In addition, increasing the number of antennas inside the cell will increase the transmit power and operating power consumption, which creates the tendency of a concave shape for EE.

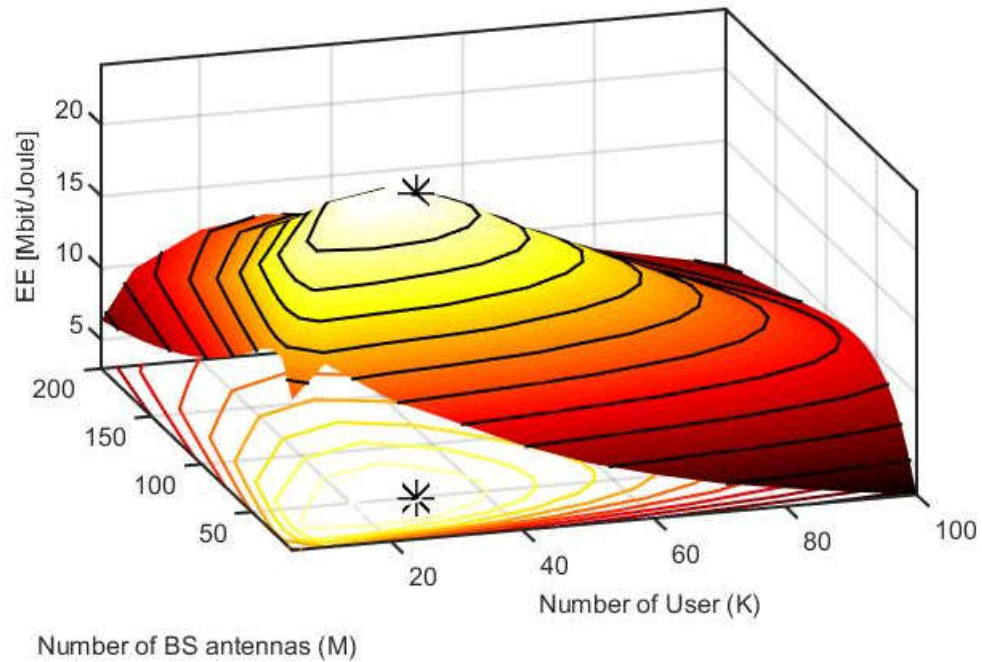


Figure 4.7: Maximum Energy Efficiency per cell as a function of number of BS (M) and number of Users (K) with MMSE Precoding Method.

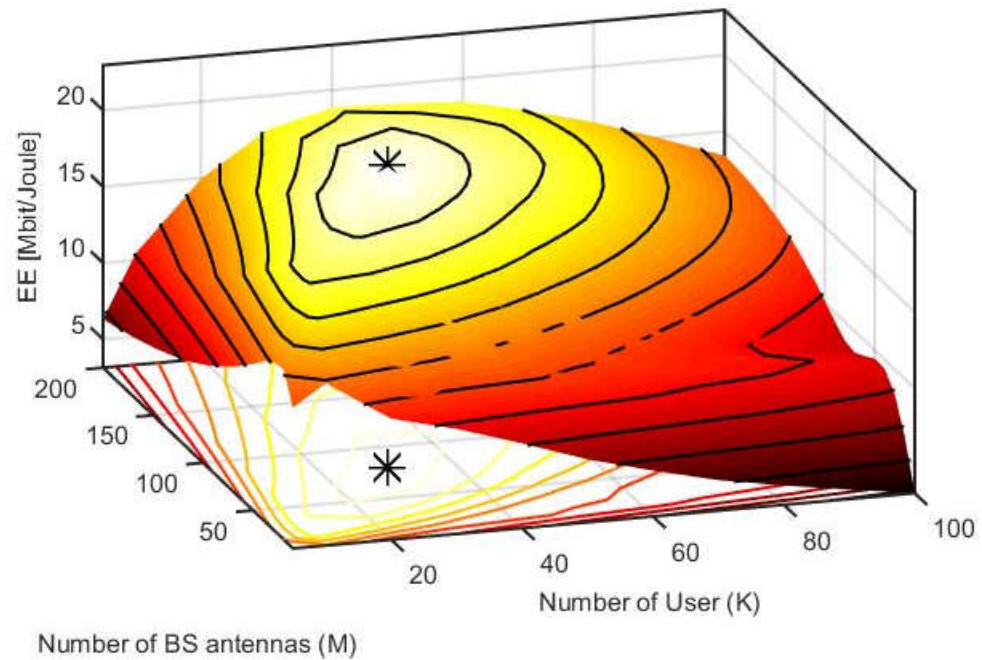


Figure 4.8: Maximum Energy Efficiency per cell as a function of number of BS (M) and number of Users (K) with ZF Precoding Method.

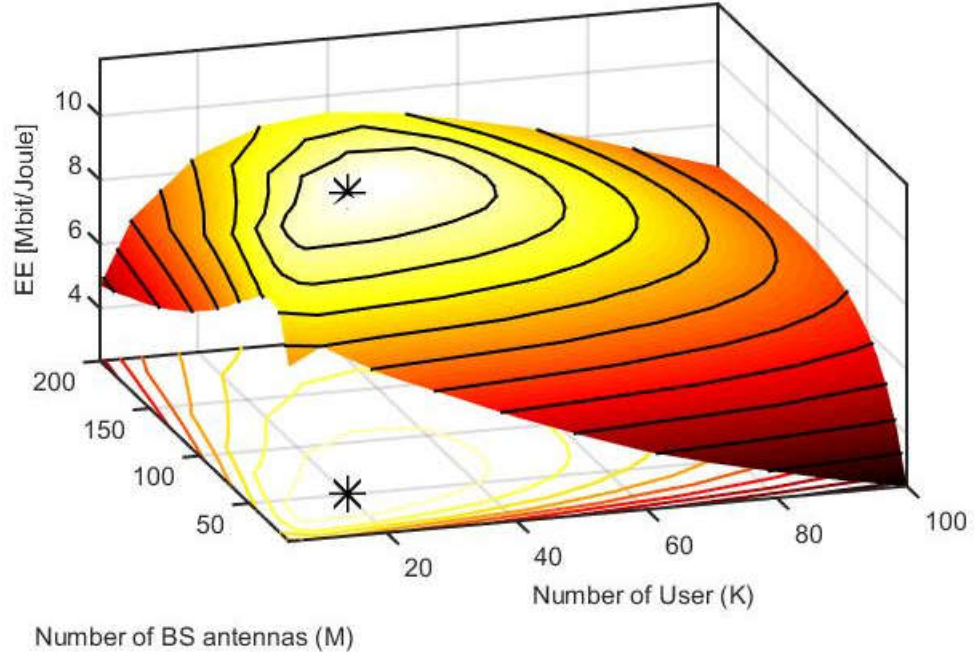


Figure 4.9: Maximum Energy Efficiency per cell as a function of number of BS (M) and number of Users (K) with MRT/MRC Precoding Method.

Table X: Comparison of Maximum EE with Reference Paper [28]:

Linear Precoding Methods		Number of antenna (M)	Number of Users (K)	Maximum Energy Efficiency [Mbit/Joule]
This Work	MMSE	50	30	24.16
	ZF	80	30	22.96
	MRT/MRC	50	20	11.77
Reference Paper [28]	MMSE	40	20	20.73
	ZF	90	30	20.25
	MRT/MRC	60	20	10.63

The explanation behind is that MRT/MRC works under strong inter-user interference, in this manner the rate per UE is small and it makes sense to plan whatever number UEs as could be allowed. The signal processing complexity is lower than with ZF for a similar M and K, but yet the power reserve funds are not sufficiently huge to adjust for the lower rates. To accomplish an indistinguishable rate from with ZF, MRT/MRC requires which would radically increase the computational/circuit power and not enhance the EE [10], [28].

Interestingly, we observe that all the EE-optimum configurations of  $(M,K)$  fall within the Massive MIMO networks, with a number of antennas in the range of tens and an antenna-UE ratio  $M/K$ . Numerical results were used in this section to find the numbers of BS antennas and UEs that jointly achieve high EE. The EE maximization problem can potentially be solved analytically with respect to  $M$  and  $K$ . Other system parameters can also be optimized. Closed-form expressions for the optimal  $(M,K)$  and transmit power were derived, from which valuable insights into the interplay between the optimization variables, hardware characteristics, and propagation environment were provided. A further leap in EE can then be achieved by adding more BS antennas to spatially multiplex UEs in every cell. The corresponding EE gains come from suppressing intra-cell interference by the many antennas and by sharing the per-cell CP costs among multiple UEs.

## Chapter 05

### Conclusion and Future Work

#### 5.1 Conclusion

Since the appearance of Massive MIMO, the system performance of wireless communication system has been improved significantly in terms of capacity, latency, reliability and etc. In this thesis,

1. We firstly analyze the background of next generation wireless communication system.
2. Introduce the massive MIMO system, power consumption model and energy efficiency.
3. And to make the system model of massive MIMO according to linear precoding methods, problem formulation solvable, we apply precoding method to address this optimization problem with number of antenna per BS and Users.
4. Finally, combining numerical results, we present that massive MIMO remarkably improves the energy efficiency.

We mainly focused on energy efficiency in massive MIMO systems. Although we have studied power allocation in uplink and downlink transmission, there are still some aspects that should be done in the future. Energy efficiency in a multiple cellular system is achieved by increasing the number of antennas at the BS. We have examined how to obtain maximum EE, which depends on selecting the optimal number of antennas and fixing the number of scheduled users inside cells. In addition, analyzing how to minimize total power consumption depends nonlinearly on  $M$  and  $K$ . Total power consumption consists of circuit power from analog devices and power amplifiers in massive MIMO systems. The techniques of linear precoding beamforming, MMSE, ZF and MRT/MRC enable minimum power transmission at the BS to select the best-performing active antenna. Consequently, linear precoding MMSE achieves maximum EE, more so than ZF and MRT, because the MMSE is able to suppress interference actively and make a massive MIMO system less sensitive to SNR at an increased number of antennas.

#### 5.2 Future Work

There are several scopes to work on energy efficiency of massive MIMO systems-

1. The energy efficiency model in these thesis only suits to single cell massive MIMO system. In the future, it can be developed to multi-cells Massive MIMO system.

2. Find other limitations of this precoding techniques and designing new precoding techniques with good overall performance in massive MIMO system.
3. Distances between users and BS are not being taken into account in this thesis. This should be considered in the future for more accurate simulation results.
4. Designing such precoding schemes can lead to promising results for FDD massive MIMO systems.

In future, we will develop a more massive MIMO system model from energy efficiency perspective, which will provide faster data transmission rate with reliable uplink and downlink wireless communication system.

## References

- [1] Wong, V., Schober, R., Ng, D., & Wang, L. (Eds.). (2017). *Key Technologies for 5G Wireless Systems*, Cambridge: Cambridge University Press. doi:10.1017/9781316771655
- [2] Qualcomm.com, 2018. *Leading the world to 5G presentation.pdf*, [Accessed: 20-Aug-2018]. Available: <https://www.qualcomm.com/qualcomm-5g-vision>
- [3] G. Fodor et al., "An Overview of Device-to-Device Communications Technology Components in METIS," in *IEEE Access*, vol. 4, no., pp.3288-3299, 2016.
- [4] Michael Grant and Stephen Boyd. CVX: Matlab software for disciplined convex programming, version 2.0 beta. Available: <http://cvxr.com/cvx>, September 2013.
- [5] "Huawei - 5G: A Technology Vision", Theparliamentmagazine.eu, 2018. [Online]. Available: <https://www.theparliamentmagazine.eu/whitepaper/clone-huawei/huawei-5g-technology-vision>. [Accessed: 20- Aug- 2018].
- [6] "Ericsson energy and carbon report", Paineira.usp.br, 2018. [Online]. Available: <http://paineira.usp.br/lassu/wp-content/uploads/2016/09/A-demonstration-of-energy-efficiency-capabilities-orchestration-in-networks.pdf>. [Accessed: 20- Aug- 2018].
- [7] S. Vishwanath, N. Jindal and A. Goldsmith, "Duality, achievable rates, and sum-rate capacity of Gaussian MIMO broadcast channels," in *IEEE Transactions on Information Theory*, vol. 49, no. 10, pp. 2658-2668, Oct. 2003.
- [8] K. N. R. S. V. Prasad and V. K. Bhargava, "Resource optimization for energy efficiency in multi-cell massive MIMO with MRC detectors," *IEEE Wireless Communications and Networking Conference Workshops (WCNCW)*, Doha, 2016, pp. 121-126.
- [9] A. Goldsmith, S. A. Jafar, N. Jindal and S. Vishwanath, "Capacity limits of MIMO channels," in *IEEE Journal on Selected Areas in Communications*, vol. 21, no. 5, pp. 684-702, June 2003.
- [10] H. Q. Ngo, E. G. Larsson and T. L. Marzetta, "Energy and Spectral Efficiency of Very Large Multiuser MIMO Systems," in *IEEE Transactions on Communications*, vol. 61, no. 4, pp. 1436-1449, April 2013.
- [11] H. Q. Ngo, M. Matthaiou and E. G. Larsson, "Performance analysis of large scale MU-MIMO with optimal linear receivers," *Swedish Communication Technologies Workshop (Swe-CTW)*, Lund, 2012, pp. 59-64.

- [12] H. Q. Ngo, M. Matthaiou and E. G. Larsson, "Massive MIMO With Optimal Power and Training Duration Allocation," in *IEEE Wireless Communications Letters*, vol. 3, no. 6, pp. 605-608, Dec. 2014.
- [13] M. Sharif and B. Hassibi, "On the capacity of MIMO broadcast channels with partial side information," in *IEEE Transactions on Information Theory*, vol. 51, no. 2, pp. 506-522, Feb. 2005.
- [15] H. Liu, H. Gao, S. Yang and T. Lv, "Low-Complexity Downlink User Selection for Massive MIMO Systems," in *IEEE Systems Journal*, vol. 11, no. 2, pp. 1072-1083, June 2017.
- [16] Björnson, Emil & Sanguinetti, Luca & Hoydis, Jakob & Debbah, Mérouane. (2015). "Optimal design of energy-efficient multi-user MIMO systems: Is massive MIMO the answer?". *IEEE Transactions on Wireless Communications*, 14. 3059-3075. 10.1109/TWC.2015.2400437
- [17] S. Mandal and S. Gauni, "Energy efficiency of single cell and multi cell Massive MIMO system MMSE estimation," *International Conference on Nextgen Electronic Technologies: Silicon to Software (ICNETS2)*, Chennai, 2017, pp. 66-70.
- [18] P. Roy, R. K. Vishwakarma, A. Jain and R. Singh, "Multiband millimeter wave antenna array for 5G communication," *International Conference on Emerging Trends in Electrical Electronics & Sustainable Energy Systems (ICETEESSES)*, Sultanpur, 2016, pp. 102-105.
- [19] H. Zhao, N. Ansari and Y. Q. Shi, "A fast non-linear adaptive algorithm for video traffic prediction," *Proceedings International Conference on Information Technology: Coding and Computing*, Las Vegas, NV, USA, 2002, pp. 54-58.
- [20] P. Krishna, T. A. Kumar and K. K. Rao, "Multiuser MIMO systems: Spectral and energy efficiencies, estimations and capacity limits," *Twelfth International Conference on Wireless and Optical Communications Networks (WOCN)*, Bangalore, India, 2015, pp. 1-6.
- [21] E. Eraslan and B. Daneshrad, "Low-Complexity Link Adaptation for Energy Efficiency Maximization in MIMO-OFDM Systems," in *IEEE Transactions on Wireless Communications*, vol. 16, no. 8, pp. 5102-5114, Aug. 2017.
- [22] Z. Luo and S. Zhang, "Dynamic Spectrum Management: Complexity and Duality," in *IEEE Journal of Selected Topics in Signal Processing*, vol. 2, no. 1, pp. 57-73, Feb. 2008.

- [23] A. Zappone, L. Sanguinetti, G. Bacci, E. Jorswieck and M. Debbah, "Energy-Efficient Power Control: A Look at 5G Wireless Technologies," in *IEEE Transactions on Signal Processing*, vol. 64, no. 7, pp. 1668-1683, April 1, 2016.
- [24] Alessio Zappone; Eduard Jorswieck, "Energy Efficiency in Wireless Networks via Fractional Programming Theory," in *Energy Efficiency in Wireless Networks via Fractional Programming Theory*, , now, 2015, pp.
- [25] C. Isheden, Z. Chong, E. Jorswieck and G. Fettweis, "Framework for Link-Level Energy Efficiency Optimization with Informed Transmitter," in *IEEE Transactions on Wireless Communications*, vol. 11, no. 8, pp. 2946-2957, August 2012.
- [26] A. Adhikary *et al.*, "Joint Spatial Division and Multiplexing for mm-Wave Channels," in *IEEE Journal on Selected Areas in Communications*, vol. 32, no. 6, pp. 1239-1255, June 2014.
- [27] Auer, Gunther & Blume, Oliver & Giannini, Vito. (2010). Energy efficiency analysis of the reference systems, areas of improvements and target breakdown. 1-68, Available: <https://www.ict-earth.eu/publications/deliverables/deliverables.html>, Nov. 2010.
- [28] Emil Björnson, Jakob Hoydis and Luca Sanguinetti (2017), "Massive MIMO Networks: Spectral, Energy, and Hardware Efficiency", *Foundations and Trends in Signal Processing*: Vol. 11, No. 3-4, pp 154–655. DOI: 10.1561/20000000093.
- [29] A. Goldsmith, S. A. Jafar, N. Jindal and S. Vishwanath, "Capacity limits of MIMO channels," in *IEEE Journal on Selected Areas in Communications*, vol. 21, no. 5, pp. 684-702, June 2003.
- [30] T. L. Marzetta, "Noncooperative Cellular Wireless with Unlimited Numbers of Base Station Antennas," in *IEEE Transactions on Wireless Communications*, vol. 9, no. 11, pp. 3590-3600, November 2010.
- [31] F. Rusek *et al.*, "Scaling Up MIMO: Opportunities and Challenges with Very Large Arrays," in *IEEE Signal Processing Magazine*, vol. 30, no. 1, pp. 40-60, Jan. 2013.
- [32] G. Auer and *et al.*, D2.3: Energy efficiency analysis of the reference systems, areas of improvements and target breakdown. INFISO-ICT-247733 EARTH, ver. 2.0, 2012. [Online]. Available: <http://www.ict-earth.eu/>

- [33] Cui, S., A. Goldsmith, and A. Bahai. "Energy-efficiency of MIMO and cooperative MIMO techniques in sensor networks".September 2004 in *IEEE Journal on Selected Areas in Communications* 22(6):1089-1098
- [34] A. Mezghani and J. A. Nossek, "Power efficiency in communication systems from a circuit perspective," *IEEE International Symposium of Circuits and Systems (ISCAS)*, Rio de Janeiro, 2011, pp. 1896-1899.
- [35] S. Tombaz, A. Vastberg and J. Zander, "Energy- and cost-efficient ultra-high-capacity wireless access," in *IEEE Wireless Communications*, vol. 18, no. 5, pp. 18-24, October 2011.
- [36] H. Yang and T. L. Marzetta, "Total energy efficiency of cellular large scale antenna system multiple access mobile networks," *2013 IEEE Online Conference on Green Communications (OnlineGreenComm)*, Piscataway, NJ, 2013, pp. 27-32.
- [37] Björnson, E., L. Sanguinetti, and M. Kountouris. 2016d. "Deploying dense networks for maximal energy efficiency: Small cells meet massive MIMO". *May 2015 IEEE Journal on Selected Areas in Communications* 34(4): 832–847
- [38] J. Hoydis, S. ten Brink and M. Debbah, "Massive MIMO in the UL/DL of Cellular Networks: How Many Antennas Do We Need?," in *IEEE Journal on Selected Areas in Communications*, vol. 31, no. 2, pp. 160-171, February 2013.
- [39] S. Boyd and L. Vandenberghe, "Numerical linear algebra background." [Online].Available: [www.ee.ucla.edu/ee236b/lectures/num-lin-alg.pdf](http://www.ee.ucla.edu/ee236b/lectures/num-lin-alg.pdf)
- [40] A. Mezghani and J. A. Nossek, "Power efficiency in communication systems from a circuit perspective," in *International Symposium on Circuits and Systems (ISCAS 2011)*, Rio de Janeiro, Brazil, May 15-19 2011,

## Appendix A

### MATLAB Function and Code

In order to obtain the performance of the discussed maximize energy efficiency techniques, some of the functions and Code used in the Matlab15a.

#### 01.Function of Compute DL and UL SE for different transmit precoding schemes

```
function [SE_MR,SE_RZF,SE_MMMSE] =  
functionComputeSE_DL_impairments(H,Hhat,C,tau_c,tau_p,nbrOfRealizations,M,K,L,p  
,rho,kappatBS,kapparUE)  
  
%Store identity matrices of different sizes  
  
eyeK = eye(K);  
eyeM = eye(M);  
  
%Compute sum of all estimation error correlation matrices at every BS  
C_totM = reshape(p*sum(sum(C,3),4),[M M L]);  
  
%Compute the pre-log factor assuming only downlink transmission  
prelogFactor = (tau_c-tau_p)/(tau_c);  
  
%Prepare to store simulation results for signal gains  
signal_MR = zeros(K,L);  
signal_ZF = zeros(K,L);  
signal_MMSE = zeros(K,L);  
  
%Prepare to store simulation results for norms of precoding vectors  
precodingNorm_MR = zeros(K,L);  
precodingNorm_ZF = zeros(K,L);  
precodingNorm_MMSE = zeros(K,L);  
  
%Prepare to store simulation results for sum interference powers  
interf_MR = zeros(K,L);
```

```

interf_ZF = zeros(K,L);
interf_MMSE = zeros(K,L);
%Prepare to store simulation results for sum impairment-caused interference
impair_MR = zeros(K,L);
impair_ZF = zeros(K,L);
impair_MMSE = zeros(K,L);
%% Go through all channel realizations
for n = 1:nbrOfRealizations
    %Go through all cells
    for j = 1:L
        %Extract channel realizations from all users to BS j
Hallj = reshape(H(:,n, :, :), [M K*L]);
        %Extract channel estimate realizations from all UEs to BS j
Hhatallj = reshape(Hhat(:,n, :, :), [M K*L]);
        %Compute MR combining in (4.11)
V_MR = Hhatallj(:,K*(j-1)+1:K*j);
        ifnargout > 1 %Compute ZF combining in (4.9)
            V_RZF = p*V_MR/(p*(V_MR'*V_MR)+eyeK);
        end
        ifnargout > 2 %Compute MMSE combining in (4.7)
            V_MMMSE = p*(p*(Hhatallj*Hhatallj')+C_totM(:, :, j)+eyeM)\V_MR;
        end
        %Go through all users in cell j
        for k = 1:K
            %%MR precoding

```

```

w = V_MR(:,k)/norm(V_MR(:,k)); %Extract precoding vector
wrep = repmat(w,[1 K*L]);

%Compute realizations of the expectations in signal and interference
signal_MR(k,j) = signal_MR(k,j) + (w'*H(:,n,k,j,j))/nbrOfRealizations;

precodingNorm_MR(k,j) = precodingNorm_MR(k,j) +
norm(w).^2/nbrOfRealizations;

interf_MR = interf_MR + rho*reshape(abs(w'*Hallj).^2,[K
L])/nbrOfRealizations;

impair_MR = impair_MR + rho*reshape(sum(abs(wrep.*Hallj).^2,1),[K
L])/nbrOfRealizations;

%%ZF precoding
ifnargout>=2
w = V_RZF(:,k)/norm(V_RZF(:,k)); %Extract precoding vector
wrep = repmat(w,[1 K*L]);

%Compute realizations of the expectations in signal and
%interference terms in (6.46)
signal_ZF(k,j) = signal_ZF(k,j) + (w'*H(:,n,k,j,j))/nbrOfRealizations;

precodingNorm_ZF(k,j) = precodingNorm_ZF(k,j) +
norm(w).^2/nbrOfRealizations;

interf_ZF = interf_ZF + rho*reshape(abs(w'*Hallj).^2,[K L])/nbrOfRealizations;

impair_ZF = impair_ZF + rho*reshape(sum(abs(wrep.*Hallj).^2,1),[K
L])/nbrOfRealizations;

end

%%MMSE precoding
ifnargout>=3
w = V_MMSE(:,k)/norm(V_MMSE(:,k)); %Extract precoding vector
wrep = repmat(w,[1 K*L]);

```

```

        %Compute realizations of the expectations in signal and interference
signal_MMSE(k,j) = signal_MMSE(k,j) + (w'*H(:,n,k,j,j))/nbrOfRealizations;

    precodingNorm_MMSE(k,j)      =      precodingNorm_MMSE(k,j)      +
    norm(w).^2/nbrOfRealizations;

    interf_MMSE      =      interf_MMSE      +      rho*reshape(abs(w'*Hallj).^2,[K
L])/nbrOfRealizations;

    impair_MMSE = impair_MMSE + rho*reshape(sum(abs(wrep.*Hallj).^2,1),[K
L])/nbrOfRealizations;

    end

    end

    end

    end

```

```

%Precompute terms that appear multiple times

```

```

sigma2 = 1/(kapparUE*kappatBS);

```

```

factor1 = 1/kapparUE;

```

```

factor2 = (1-kappatBS)/(kapparUE*kappatBS);

```

```

%Compute SEs according to Theorem 6.5 and (6.46)

```

```

SE_MR = prelogFactor*real(log2(1+(rho*abs(signal_MR).^2) ./ (factor1*interf_MR +
factor2*impair_MR - rho*abs(signal_MR).^2 + sigma2)));

```

```

ifnargout>=2

```

```

    SE_ZF = prelogFactor*real(log2(1+(rho*abs(signal_ZF).^2) ./ (factor1*interf_ZF +
factor2*impair_ZF - rho*abs(signal_ZF).^2 + sigma2)))

```

```

;end

```

```

ifnargout>=3

```

```

    SE_MMSE      =      prelogFactor*real(log2(1+(rho*abs(signal_MMMSE).^2)      ./
(factor1*interf_MMSE      +      factor2*impair_MMSE      -      rho*abs(signal_MMSE).^2
+sigma2)));

```

```

end

```

## 02.Function of Compute the UL and DL Power

```

function [channelGains_MR,channelGains_RZF,channelGains_MMMSE] =
functionComputeULDLPowerLevels(H,Hhat,C,nbrOfRealizations,M,K,L,p)

%Store identity matrices of different sizes

eyeK = eye(K);

eyeM = eye(M);

%Compute sum of all estimation error correlation matrices at every BS

C_totM = reshape(p*sum(sum(C(:,:,:,3),4),[M M L]));

%Prepare to store simulation results

channelGains_MR = zeros(K,L,K,L);

channelGains_ZF = zeros(K,L,K,L);

channelGains_MMSE = zeros(K,L,K,L);

%% Go through all channel realizations

for n = 1:nbrOfRealizations

    %Go through all cells

    for j = 1:L

        %Extract channel estimate realizations from all UEs to BS j

Hallj = reshape(H(:,n,:,:),[M K*L]);

        %Extract channel estimate realizations from UEs in cell j to BS j

Hhatallj = reshape(Hhat(:,n,:,:),[M K*L]);

        %Compute three different combining/precoding schemes

V_MR = Hhatallj(:,K*(j-1)+1:K*j); %MR in Eq. (XX)

V_ZF = p*V_MR/(p*(V_MR'*V_MR)+eyeK); %RZF in Eq. (XX)

V_MMSE = p*(p*(Hhatallj*Hhatallj')+C_totM(:,j)+eyeM)\V_MR; %MMSE in
Eq. (XX)

        %Go through all UEs in cell j
    end
end

```

```

for k = 1:K
    %%MR combining/precoding
    v = V_MR(:,k); %Extract combining vector
    v = v/norm(v);
    %Compute UL powers for the interfering channels from all UEs to
    %UE k in cell j. These are also the interfering DL gains
    %from UE k in cell j to all other UEs.
    channelGains_MR(k,j,,:) = channelGains_MR(k,j,,:) + reshape(abs(v'*Hallj).^2,[1 1 K
    L])/nbrOfRealizations;
    %%ZF combining/precoding
    v = V_ZF(:,k); %Extract combining vector
    v = v/norm(v);
    %Compute UL powers for the interfering channels from all UEs to
    %UE k in cell j. These are also the interfering DL gains
    %from UE k in cell j to all other UEs.
    channelGains_ZF(k,j,,:) = channelGains_RZF(k,j,,:) + reshape(abs(v'*Hallj).^2,[1 1 K
    L])/nbrOfRealizations;
    %%M-MMSE combining/precoding
    v = V_MMSE(:,k); %Extract combining vector
    v = v/norm(v);
    %Compute UL powers for the interfering channels from all UEs to
    %UE k in cell j. These are also the interfering DL gains
    %from UE k in cell j to all other UEs.
    channelGains_MMMSE(k,j,,:) = channelGains_MMSE(k,j,,:) +
    reshape(abs(v'*Hallj).^2,[1 1 K L])/nbrOfRealizations;
end

```

end

end

### 03.Function of the CP model Coefficients

```
function [P_FIX,P_LO,P_BS,P_UE,P_COD,P_DEC,L_BS,P_BT] =  
functionCPmodel(valueset)  
  
%% Define parameter values for Value  
  
if  
  
    P_FIX = 10;  
  
    P_LO = 0.2;  
  
    P_BS = 0.4;  
  
    P_UE = 0.2;  
  
    P_COD = 0.1*10^(-9);  
  
    P_DEC = 0.8*10^(-9);  
  
    L_BS = 75*10^9;  
  
    P_BT = 0.25*10^(-9);  
  
end
```

### 04.Function of the total CP computation with different processing schemes

```
function [P_MR,P_RZF,P_MMMSE,P_ZF,P_SMMSE] =  
functionCPcomputation(Mrange,K,L,B,tau_c,tau_p,valueset,sumSE_MR,sumSE_RZF,su  
mSE_MMMSE,sumSE_ZF,sumSE_SMMSE)  
  
%Obtain CP model  
  
[P_FIX,P_LO,P_BS,P_UE,P_COD,P_DEC,L_BS,P_BT] = functionCPmodel(valueset);  
  
%Prepare to store simulation results  
  
P_MR = zeros(length(Mrange),1);  
  
P_TC = zeros(length(Mrange),1);
```

```

P_CE = zeros(length(Mrange),1);
P_SP_RT = zeros(length(Mrange),1);
P_SP_DL = zeros(length(Mrange),1);
P_SP_UL_MR = zeros(length(Mrange),1);
%Compute CP for coding and decoding using (5.35)
P_CD_MR = (P_COD + P_DEC)*B*sumSE_MR;
%Compute CP for backhaul traffic using (5.36)
P_BH_MR = P_BT*B*sumSE_MR;
%Repeat computations for MMSE
if nargin>9
    P_MMSE = zeros(length(Mrange),1);
    P_CD_MMSE = (P_COD + P_DEC)*B*sumSE_MMSE;
    P_BH_MMSE = P_BT*B*sumSE_MMSE;
    P_SP_UL_MMSE = zeros(length(Mrange),1);
end
%Repeat computations for ZF
if nargin>10
    P_ZF = zeros(length(Mrange),1);
    P_CD_ZF = (P_COD + P_DEC)*B*sumSE_ZF;
    P_BH_ZF = P_BT*B*sumSE_ZF;
    P_SP_UL_ZF = zeros(length(Mrange),1);
end
%Go through all number of antennas
for index = 1:length(Mrange)
    %Extract current number of antennas

```

```

M = Mrange(index);

%Compute CP for transceiver chains
P_TC(index) = M*P_BS + P_LO + K*P_UE;

%Compute CP for channel estimation with all other schemes, where only
%the channels to UEs in other cells are estimated
P_CE(index) = 3*K*B/(tau_c*L_BS)*(M*tau_p + M^2);

%Compute CP for UL reception and DL transmission
P_SP_RT(index) = (tau_c - tau_p)*3*B/(tau_c*L_BS)*M*K;

%Compute CP for computation of precoding vectors
P_SP_DL(index) = 4*M*K*B/(tau_c*L_BS);

%Sum up the power terms that are independent of the processing scheme
P_SAME = P_FIX + P_TC(index) + P_SP_RT(index) + P_SP_DL(index);

%Compute CP for computation of the combining vectors with different schemes
P_SP_UL_MR(index) = 7*B*K/(tau_c*L_BS);

%Compute the final CP values
P_MR(index) = P_SAME + P_CE(index) + P_CD_MR(index) + P_BH_MR(index) +
P_SP_UL_MR(index);

%Repeat same computations for MMSE
if nargin>9
    P_SP_UL_MMSE(index) = 3*B*(L*(3*M^2 + M)*K/2 + M^3/3 + 2*M +
M*tau_p*(tau_p-K))/(tau_c*L_BS);

    P_MMSE(index) = P_SAME + P_CE(index) + P_CD_MMSE(index) +
P_BH_MMSE(index) + P_SP_UL_MMSE(index);
end

%Repeat same computations for ZF
if nargin>10

```

$P_{SP\_UL\_ZF}(\text{index}) = 3*B*(3*K^2*M/2 + M*K/2 + (K^3 - K)/3 + (7/3)*K)/(\tau_c*L_{BS});$

$P_{ZF}(\text{index}) = P_{SAME} + P_{CE}(\text{index}) + P_{CD\_ZF}(\text{index}) + P_{BH\_ZF}(\text{index}) + P_{SP\_UL\_ZF}(\text{index});$

end

end

## 05. Function of Compute Maximize Energy Efficiency

```
function [EE,rate,power] =
functionEnergyEfficiency(power,h,etaUE,etaBS,noise,R,kappaUE,kappaBS,omega,rho,z
eta,trafficPortion,ULDLratio)
```

%A typical pilot signal

d = sqrt(power);

%Extract number of antennas

N = size(h,1);

%Extract number of Monte Carlo simulations

nbrOfMonteCarloRealizations = size(h,2);

%Compute matrix A in the LMMSE estimator (see Eq. (9))

$A_{MMSE} = \text{conj}(d) * R / (\text{abs}(d)^2*(1+kappaUE)*R + \text{abs}(d)^2*kappaBS*\text{diag}(\text{diag}(R))+\text{eye}(N));$

%Placeholders for storing Monte Carlo simulation results

firstMoment = zeros(nbrOfMonteCarloRealizations,1);

distortionTerm = zeros(nbrOfMonteCarloRealizations,1);

%Go through all Monte Carlo realizations

for k = 1:nbrOfMonteCarloRealizations

%Compute received signal

$z = h(:,k) * (d + d*\eta_{UE}(k)) + d*\eta_{BS}(:,k) + \text{noise}(:,k);$

%Compute channel estimates

```

hhat = A_MMSE*z;

%Compute the beamforming vector (MRT/MRC)

beamforming = sqrt(power)*hhat/norm(hhat);

%Compute a realization of the first moment of the inner product between beamforming
and channel

firstMoment(k) = h(:,k)*beamforming;

distortionTerm(k) = sum( (abs(h(:,k)).^2) .* (abs(beamforming).^2));

end

%Finalize the Monte Carlo simulations by computing lower bounds on the capacity

rate = trafficPortion * log2(1+ abs(mean(firstMoment,1)).^2 ./ ( (1+kappaUE) *
var(firstMoment) + kappaUE* abs(mean(firstMoment,1)).^2 +
kappaBS*mean(distortionTerm,1) + 1) );

%Compute the energy efficiency according to Definition 1

EE = rate/((power/omega + N*rho + zeta)*ULDLratio);

```

## 06. Complexity of Computing Combining Matrix

```

close all;

clear;

tau_c = 400; %Select length of coherence block

Mrange = 10:10:200; %Define range of number of BS antenna

Krange = 1:100; %Define range of number of UEs

L = 5; %Set number of cells considered in the MMSE scheme

%% Consider M=100 and varying K

K = Krange;

M = max(Mrange);

tau_u = (tau_c-K); %Compute number of samples for uplink data

receiverProcessing = tau_u.*K*M; %Compute complexity of receive combining

```

```

%Add complexity of computing combining matrix

complexity_MMMSE = receiverProcessing + L*K*(M^2+M)/2 + M^2*K + (M^3-M)/3;
%M-MMSE

complexity_ZF = receiverProcessing + 3*K.^2*M/2 + M*K/2 + (K.^3-K)/3; %ZF

complexity_MR = receiverProcessing; %MR

%Plot the simulation results for M=100 and varying K

figure(1);

grid on;

hold on;

box on;

plot(K,complexity_MMSE,'r-','LineWidth',1);

plot(K,complexity_ZF,'g--','LineWidth',1);

plot(K,complexity_MR,'b-','LineWidth',1);

plot(K([1 5:5:100]),complexity_MMSE([1 5:5:100]),'rd-','LineWidth',1);

plot(K([1 5:5:100]),complexity_MR([1 5:5:100]),'bs-','LineWidth',1);

plot(K([1 5:5:100]),complexity_ZF([1 5:5:100]),'gh--','LineWidth',1);

xlabel('Number of UEs (K)');

ylabel('Number of complex multiplications');

legend('MMSE','ZF','MR','Location','NorthWest');

%% Consider K=10 and varying M

K = Krange(10);

M = Mrange;

tau_u = (tau_c-K); %Compute number of samples for uplink data

receiverProcessing = tau_u*K*M; %Compute complexity of receive combining

%Add complexity of computing combining matrix

```

```

complexity_MMMSE = receiverProcessing + L*K*(M.^2+M)/2 + M.^2*K + (M.^3-
M)/3;

complexity_ZF = receiverProcessing + 3*K^2*M/2 + M*K/2 + (K^3-K)/3;

complexity_MR = receiverProcessing;

%Plot the simulation results for K=10 and varying M

figure(2);

grid on;

hold on;

box on;

plot(M,complexity_MMSE,'rd-','LineWidth',1);

plot(M,complexity_ZF,'gh--','LineWidth',1);

plot(M,complexity_MR,'bs-','LineWidth',1);

xlabel('Number of antennas (M)');

ylabel('Number of complex multiplications');

legend('MMSE','ZF','MR','Location','NorthWest');

```

### **07. Compute the total CP Power with number of Antenna**

```

close all;

clear;

load section5_Mvarying_K10_20; %Load simulation data

%Number of UEs per BS

k_index = 1;

K = Krange(k_index);

%Fractions of data samples used for UL and DL

ULfraction = 1/3;

DLfraction = 2/3;

```

```

%Compute joint UL/DL sum SE using the fractions of UL/DL data

sumSE_MMSE      =      ULfraction*sumSE_MMMSE_UL(:,k_index)      +
DLfraction*sumSE_MMMSE_DL(:,k_index);

sumSE_ZF        =      ULfraction*sumSE_ZF_UL(:,k_index)        +
DLfraction*sumSE_ZF_DL(:,k_index);

sumSE_MR        =      ULfraction*sumSE_MR_UL(:,k_index)        +
DLfraction*sumSE_MR_DL(:,k_index);

L = 16; %Number of BSs

B = 20e6; %Communication bandwidth

tau_c = 450; %Select length of coherence block

tau_p = K; %Select length of pilot sequences

%Prepare to store simulation results

P_MMSE = zeros(length(Mrange),2);

P_ZF = zeros(length(Mrange),2);

P_MR = zeros(length(Mrange),2);

%% Compute CP values for different value sets

forvalueset = 1

[P_MR(:,valueset),P_ZF(:,valueset),P_MMSE(:,valueset)]=functionCPcomputation(Mra
nge,K,L,B,tau_c,tau_p,valueset,sumSE_MR,sumSE_ZF,sumSE_MMSE);

End

%% Plot the simulation results

grid on;

hold on;

box on;

forvalueset = 1

plot(Mrange,10*log10(P_MMSE(:,valueset)/0.001),'rd-','LineWidth',1);

plot(Mrange,10*log10(P_ZF(:,valueset)/0.001),'gh--','LineWidth',1);

```

```

plot(Mrange,10*log10(P_MR(:,valueset)/0.001),'bp','LineWidth',1);
end
xlabel('Number of antennas (M)');
ylabel('Total CP [Watt]');
legend('MMSE','ZF','MR','Location','SouthEast');

```

### **08. Compute the total CP Power with number of Users**

```

close all;
clear;
load section5_M100_Kvarying; %Load SE simulation data
%Fractions of data samples used for UL and DL
ULfraction = 1/3;
DLfraction = 2/3;
%Compute joint UL/DL sum SE using the fractions of UL/DL data
sumSE_MMSE = ULfraction*sumSE_MMSE_UL + DLfraction*sumSE_MMSE_DL;
sumSE_ZF = ULfraction*sumSE_ZF_UL + DLfraction*sumSE_ZF_DL;
sumSE_MR = ULfraction*sumSE_MR_UL + DLfraction*sumSE_MR_DL;
L = 16; %Number of BSs
M = 200; %Number of BS antennas
B = 20e6; %Communication bandwidth
tau_c = 400; %Select length of coherence block
tau_p = Krange; %Select length of pilot sequences
%Prepare to store simulation results
P_MMSE = zeros(length(Krange),2);
P_ZF = zeros(length(Krange),2);
P_MR = zeros(length(Krange),2);

```

```

%% Compute CP values for different value sets 1
for valueset = 1 %1:2
    for k = 1:length(Krange)
        %Compute the total CP with different schemes
        [P_MR(k,valueset),P_ZF(k,valueset),P_MMSE(k,valueset)]=functionCPcomputation(M,
        Krange(k),L,B,tau_c,tau_p(k),valueset,sumSE_MR,sumSE_MMSE,sumSE_ZF);
            end
        end
    %% Plot the simulation results
    grid on;
    hold on;
    box on;
    for valueset = 1
        plot(Krange,10*log10(P_MMSE(:,valueset)/0.001),'rd-','LineWidth',1);hold on;
        plot(Krange,10*log10(P_ZF(:,valueset)/0.001),'gh--','LineWidth',1);
        plot(Krange,10*log10(P_MR(:,valueset)/0.001),'bp-','LineWidth',1);
        end
    xlabel('Number of UEs (K)');
    ylabel('Total CP [Watt]');
    legend('MMSE','ZF','MR','Location','NorthWest');

```

### **09.Power Consumption vs. Throughput**

```

close all;
clear;
%Load SE simulation data, generated using the code from Section 4
load section5_Mvarying_K10_20;
k_index = 1; %Selecting K = 10 from the loaded SE results

```

```

K = Krange(k_index);

%Fractions of data samples used for UL and DL
ULfraction = 1/6; %1/3
DLfraction = 2/6; %2/3

%Compute joint UL/DL sum SE using the fractions of UL/DL data
sumSE_MMSE      =      ULfraction*sumSE_MMSE_UL(:,k_index)      +
DLfraction*sumSE_MMMSE_DL(:,k_index);

sumSE_ZF        =      ULfraction*sumSE_ZF_UL(:,k_index)        +
DLfraction*sumSE_ZF_DL(:,k_index);

sumSE_MR        =      ULfraction*sumSE_MR_UL(:,k_index)        +
DLfraction*sumSE_MR_DL(:,k_index);

%Number of BSs
L = 16; %16

%Communication bandwidth
B = 20e6;

%PA efficiency UEs and BSs
mu_UE = 0.4;
mu_BS = 0.5;

%Define the pilot reuse factor
f = 1;

%Select length of coherence block
tau_c = 200;

%Compute length of pilot sequences
tau_p = f*K;

%Transmit power per UE in W
p = 0.1;

```

```

%Compute total effective transmit power

ETP_total=      K*p*(tau_p/mu_UE  +  (tau_c-tau_p)*(ULfraction/mu_UE  +
DLfraction/mu_BS))/tau_c;

%Compute the total CP with different schemes

[P_MR,P_MMSE,P_ZF]
functionCPcomputation(Mrange,K,L,B,tau_c,tau_p,valueset,sumSE_MR,sumSE_MMSE
,sumSE_ZF);

%Compute EE with M-MMSE

EE_MMMSE = (B*sumSE_MMMSE)./(ETP_total + P_MMMSE);

%Compute EE with ZF

EE_ZF = (B*sumSE_ZF)./(ETP_total + P_ZF);

%Compute EE with MR

EE_MR = (B*sumSE_MR)./(ETP_total + P_MR);

%Plot simulation results

figure;

hold on;

plot(B*sumSE_MMSE/10^6,EE_MMSE/10^6, 'rd-','LineWidth',1);

plot(B*sumSE_ZF/10^6,EE_ZF/10^6,'rs--','LineWidth',1);

plot(B*sumSE_MR/10^6,EE_MR/10^6,'bs-','LineWidth',1);

xlabel('Throughput [Mbit/s/cell]');

ylabel('Power Consumption [Joule/s/cell]');

legend('M-MMSE','RZF','MR','Location','NorthWest');

10.Average UL and DL sum SE

close all;

clear;

L = 16; %Number of BSs

```

```

K = 10; %Number of UEs per BS

Mrange = 10:10:210; %Define the range of BS antennas

%Mrange = 10:10:100;

Mmax = max(Mrange); %Extract maximum number of BS antennas

fRange = 1;

%Select the number of setups with random UE locations

nbrOfSetups = 1; %100

%Select the number of channel realizations per setup

nbrOfRealizations = 1; %100

B = 20e6;

%Total uplink transmit power per UE (mW)

p = 100;

noiseFigure = 7;

noiseVarianceDbm = -174 + 10*log10(B) + noiseFigure;

tau_c = 400;

%Use the approximation of the Gaussian local scattering model

accuracy = 2;

%Angular standard deviation in the local scattering model (in degrees)

ASDdeg = 10;

%Prepare to save simulation results

sumSE_MR = zeros(length(Mrange),length(fRange),nbrOfSetups);

sumSE_ZF = zeros(length(Mrange),length(fRange),nbrOfSetups);

sumSE_MMMSE = zeros(length(Mrange),length(fRange),nbrOfSetups);

%% Go through all setups

for n = 1:nbrOfSetups

```

```

%Output simulation progress
disp([num2str(n) ' setups out of ' num2str(nbrOfSetups)]);

%Compute channel statistics for one setup
[R,channelGaindB] = functionExampleSetup(L,K,Mmax,accuracy,ASDdeg);

%Compute the normalized average channel gain, where the normalization
%is based on the noise power
channelGainOverNoise = channelGaindB - noiseVarianceIndB;

%Go through all number of antennas
for m = 1:length(Mrange)

    %Output simulation progress
    disp([num2str(m) ' antennas out of ' num2str(length(Mrange))]);

    %Go through all pilot reuse factors
    for s = 1:length(fRange)

        %Extract pilot reuse factor
        f = fRange(s);

        %Generate channel realizations with estimates and estimation error correlation matrices
        [Hhat,C,tau_p,Rscaled] =
functionChannelEstimates(R(1:Mrange(m),1:Mrange(m),:,:),channelGainOverNoise,nbr
OfRealizations,Mrange(m),K,L,p,f);

        %Compute SEs
        [SE_MR,SE_ZF,SE_MMSE] =
functionComputeSE_UL(Hhat,C,Rscaled,tau_c,tau_p,nbrOfRealizations,Mrange(m),K,L,
p);

        %Save average sum SE per cell
sumSE_MR(m,s,n) = mean(sum(SE_MR,1));
sumSE_ZF(m,s,n) = mean(sum(SE_ZF,1));
sumSE_MMMSE(m,s,n) = mean(sum(SE_MMMSE,1));

```

```

clearHhat C Rscaled;

end

end

    %Delete large matrices

clear R;

end

%% Plot the simulation results

for s = 1:length(fRange)

figure;

grid on;

hold on;

box on;

plot(Mrange,mean(sumSE_MMMSE(:,s,:),3),'rd-','LineWidth',1);

plot(Mrange,mean(sumSE_ZF(:,s,:),3),'rh--','LineWidth',1);

plot(Mrange,mean(sumSE_MR(:,s,:),3),'bs-','LineWidth',1);

xlabel('Number of antennas (M)');

ylabel('Average sum SE [bit/s/Hz/cell]');

legend('M-MMSE','ZF','MR','Location','NorthWest');

ylim([0 80]);

end

```

## **11. Compute Maximum Energy Efficiency with Different Precoding Methods**

```

close all;

clear;

valueset = 1;

```

```

%Load SE simulation data
load section5_Mvarying_Kvarying.mat;
L = 16; %Number of BSs
B = 20e6;
mu_UE = 0.6;
mu_BS = 0.75;
f= 1;
tau_c = 400;
%Fractions of data samples used for UL and DL
ULfraction = 1/3;
DLfraction = 2/3;
p = 0.01;;
%Compute joint UL/DL sum SE using the fractions of UL/DL data
sumSE_MMSE = ULfraction*sumSE_MMSE_UL + DLfraction*sumSE_MMSE_DL;
sumSE_ZF = ULfraction*sumSE_ZF_UL + DLfraction*sumSE_ZF_DL;
sumSE_MR = ULfraction*sumSE_MR_UL + DLfraction*sumSE_MR_DL;
%Prepare to save simulation results
EE_MR = zeros(length(Mrange),length(Krange));
EE_ZF = zeros(length(Mrange),length(Krange));
EE_MMMSE = zeros(length(Mrange),length(Krange));
%% Go through all number of BS antennas
for m = 1:length(Mrange)
    %Go through all number of UEs
    for k = 1:length(Krange)
        %Compute length of pilot sequences

```

```

tau_p = f*Krange(k);

    %Compute the total CP with different schemes

    [P_MR,P_ZF,P_MMSE]
functionCPcomputation(Mrange(m),Krange(k),L,B,tau_c,tau_p,valueSet,sumSE_MR,su
mSE_ZF,sumSE_MMSE);

    %Compute total effective transmit power

ETP_total=    Krange(k)*p*(tau_p/mu_UE  +  (tau_c-tau_p)*(ULfraction/mu_UE  +
DLfraction/mu_BS))/tau_c;

    %Compute EE with MR

EE_MR(m,k) = (B*sumSE_MR(m,k))./(ETP_total + P_MR);

    %Compute EE with ZF

EE_ZF(m,k) = (B*sumSE_ZF(m,k))./(ETP_total + P_ZF);

    %Compute EE with MMSE

EE_MMMSE(m,k) = (B*sumSE_MMSE(m,k))./(ETP_total + P_MMSE);

end

end

%% Plot simulation results

figure;

hold on;

box on;

grid on;

surf(Krange,Mrange,EE_MMSE/10^6,'EdgeColor','none');

colormap hot

shadinginterp

hold on

contour3(Krange,Mrange,EE_MMSE/1e6,10,'k')

```

```

[~,I] = max(EE_MMMSE(:));
[row,col] = ind2sub(size(EE_MMSE),I);
Kopt = Krange(col); %Optimal number of UEs
Mopt = Mrange(row); %Optimal number of BS antennas
hold on
plot3(Kopt,Mopt,EE_MMSE(row,col)/1e6,'k*','MarkerSize',16,'MarkerFaceColor','black'
);
hold on
plot3(Kopt,Mopt,min(min(EE_MMSE))/1e6,'k*','MarkerSize',16,'MarkerFaceColor','black'
);
view([-17 32]);
xlabel('Number of UEs (K)')
ylabel('Number of BS antennas (M)');
zlabel('EE [Mbit/Joule]');
%Plot Figure MAX EE of ZF
figure;
hold on;
box on;
grid on;
surf(Krange,Mrange,EE_ZF/10^6,'EdgeColor','none');
colormap hot
shadinginterp
hold on
contour3(Krange,Mrange,EE_ZF/1e6,10,'k')
[~,I] = max(EE_ZF(:));
[row,col] = ind2sub(size(EE_RZF),I);

```

```

Kopt = Krange(col); %Optimal number of UEs
Mopt = Mrange(row); %Optimal number of BS antennas
hold on
plot3(Kopt,Mopt,EE_ZF(row,col)/1e6,'k*','MarkerSize',16,'MarkerFaceColor','black');
hold on
plot3(Kopt,Mopt,min(min(EE_ZF))/1e6,'k*','MarkerSize',16,'MarkerFaceColor','black');
view([-17 32]);
xlabel('Number of UEs (K)')
ylabel('Number of BS antennas (M)');
zlabel('EE [Mbit/Joule]');
%Plot Figure MAX EE of MR
figure;
hold on;
box on;
grid on;
surf(Krange,Mrange,EE_MR/10^6,'EdgeColor','none');
colormap hot
shadinginterp
hold on
contour3(Krange,Mrange,EE_MR/1e6,10,'k')
[EE_max,I] = max(EE_MR(:));
[row,col] = ind2sub(size(EE_MR),I); %2D maximizer
Kopt = Krange(col); %Optimal number of UEs
Mopt = Mrange(row); %Optimal number of BS antennas
hold on

```

```
plot3(Kopt,Mopt,EE_MR(row,col)/1e6,'k*','MarkerSize',16,'MarkerFaceColor','black');  
hold on  
plot3(Kopt,Mopt,min(min(EE_MR))/1e6,'k*','MarkerSize',16,'MarkerFaceColor','black');  
view([-17 32]);  
xlabel('Number of UEs (K)')  
ylabel('Number of BS antennas (M)');  
zlabel('EE [Mbit/Joule]');
```